Gregor Paster, BSc

Investigation and kinetic modeling of biphasic esterification of acetic acid with 1-octanol

Master Thesis

for the Attainment of the Degree

Master of Science

Course of Study

Chemical and Process Engineering

Graz University of Technology

Supervisor

Ass.Prof. Dipl.-Ing. Dr.techn. Susanne Lux

Institute of Chemical Engineering and Environmental Technology

Graz, July 2020

Eidesstattliche Erklärung

Ich erkläre an Eides statt, dass ich die vorliegende Arbeit selbstständig verfasst, andere als die angegebenen Quellen/Hilfsmittel nicht benutzt und die den benutzten Quellen wörtlich und inhaltlich entnommenen Stellen als solche kenntlich gemacht habe. Das in TUGRAZonline hochgeladene Textdokument ist mit der vorliegenden Masterarbeit identisch.

Datum, Unterschrift

Acknowledgements

The author would like to acknowledge the great support from his supervisor *Prof. Dr. Susanne Lux* and from his Co-advisor *Dr. Andreas Toth*.

Abstract

Among other low molecular weight carbon acids, acetic acid is produced during pulping of wood as a byproduct in low concentrated aqueous solutions. An effective method for recovering these substances should be developed for enabling a further utilization of this resource. Reactive extraction with esterification as chemical reaction could be a suitable method for this issue. The reaction kinetics of this method is essential for understanding the process and further investigations. In this task, an experimental investigation on kinetics of the system was done. The aqueous feed was simplified to a 1 mol L^{-1} solution of acetic acid in deionized water. The analyzed solvent was 1-octanol with dissolved metallosurfactant $NiDBSA_2$ as catalyst. The catalyst was synthesized from $Ni(OH)_2$ and 4-Dodecylbenzenesulfonic acid. Reaction kinetics of the reactive extraction were analyzed at two catalyst loads of 5 wt% and 20 wt% at three temperatures (25, 40, 60 °C) in a batch setup. A volume ratio of organic to aqueous phase equal to 1 was used for all investigations. Kinetic modeling of biphasic reactive systems was done by assuming a quasi-monophasic system. Order of catalyst, reaction rate constant and parameters of the liquid-liquid equilibrium of main acetic acid were determined. The model shows an accurate performance at all analyzed combinations of temperatures and mass fractions of catalyst. At 60 °C and 20 wt% catalyst, a maximum conversion of approximately 57 % after 300 minutes was determined, while 67 % of total acetic acid was recovered by esterification and additional physical extraction. The equilibrium conversion at 40 and 60 °C was determined as approximately 65 %.

Key words: acetic acid, reactive extraction, 1-octanol, surfactant, order of catalyst

Kurzfassung

Neben anderen niedermolekularen Carbonsäuren wird Essigsäure in Verfahrensprozessen der Papier- und Zellstoffproduktion als Nebenprodukt in niedrigkonzentrierten wässrigen Lösungen erzeugt. Ein effektives Verfahren zur Abtrennung von Essigsäure ist nötig, um diese als Rohstoff nutzbar zu machen. Reaktivextraktion mit Veresterung als chemische Reaktion ist eine Lösung, die sich bereits in vorangegangen Untersuchungen als vielversprechend erwiesen hat. Die Beschreibung der Reaktionskinetik für diese Reaktivextraktion ist essentiell für weitere Forschung und wurde in dieser Arbeit untersucht. Die verwendete Lösungsmittelphase setzte sich aus 1-Octanol und dem gelösten Metalltensid $NiDBSA_2$ als Katalysator zusammen. Der Katalysator wurde aus $Ni(OH)_2$ und 4-Dodecylbenzylsulfonsäure hergestellt. Katalysatorbeladungen von 5 gew% und 20 gew% wurden bei 25, 40 und 60 °C in einem Batchsystem untersucht. Die wässrige Feedphase wurde vereinfacht als 1 molare Essigsäurelösung angenommen. Als Volumenverhältnis der beiden Phasen wurde 1 gewählt. Für die kinetische Modellierung wurde ein quasi-einphasiges System angenommen. Die Ordnung des Katalysators, Verteilungsgleichgewichte und die Reaktionskonstanten der jeweiligen Temperaturen bezogen auf Essigsäure konnten berechnet werden. Das kinetische Modell zeigt gute Ergebnisse bei allen untersuchten Temperaturen und Katalysatorbeladungen. Bei 60 °C und 20 gew% $NiDBSA_2$ konnte ein maximaler Umsatz von etwa 57 % nach 300 Minuten ermittelt werden. In dieser Zeit konnten 67 % der gesamten Essigsäure durch Versterung zu Octylacetat und zusätzliche physikalische Extraktion rückgewonnen werden. Der Gleichgewichtsumsatz bei 40 und 60 °C stellte sich bei etwa 65 % ein.

Key words: Essigsäure, Reaktivextraktion, 1-Octanol, Tensid, Katalysatorordnung

Table of Contents

Dictionary

Symbols	Description	Unit
c	Concentration	mol L^{-1}
k_1	Forward reaction rate constant	L mol^{-1} min^{-1}
k_2	Backward reaction rate constant	min^{-1}
m	Mass	g
n	Molar amount	mol
r	Reaction rate	mol L^{-1} min^{-1}
rat	Mass fraction ratio of 1-octanol to n-undecane	
t	Time	min
w	Mass fraction	
CMC	Critical micelle concentration	mol L^{-1}
E	Error in mass balance	
K_D	Distribution coefficient	$\frac{\text{mol org}}{\text{mol aqu}}$
K	Equilibrium constant of chemical reaction	L mol^{-1}
L	Molar load	$\frac{\text{mol HAc+OctAc}}{\text{mol Oct+OctAc}}$
M	Molar mass	g mol^{-1}
R	Recovery	
T	Temperature	°C
V	Volume	mL
X	Conversion	
γ	Order of catalyst	
ρ	Density	g mL^{-1}
$\sigma_{interface}$	Interfacial tension	mN m^{-1}
σ_S	Surface tension	mN m^{-1}

Abbreviations	Description
aqu	Aqueous phase
cat	Catalyst ($NiDBSA_2$)
fin	Final, after 300 minutes
mono	quasi-monophasic
org	Organic phase
tr	Transferred
DBSA	4-Dodecylbenzenesulfonic acid
Eq	Equilibrium
GC	Gas chromatography
HAc	Acetic acid
KF	Karl Fischer titration
LLE	Liquid-liquid-equilibrium
$Ni(OH)_2$	Nickel(II) hydroxide
$NiDBSA_2$	4-Dodecylbenzenesulfonic acid Nickel (II) salt
Oct	1-octanol
OctAc	Octyl acetate
Und	*n*-undecane
W	Water

1 Introduction

In these days, climate change is probably the most urgent problem for mankind. The usage of fossil resources as crude oil and gas or coal is enhancing the problem, because they are mainly burned to CO_2 for generation of energy. In the chemical industry fossil resources are used to produce standard chemicals, plastics or intermediate products. If fossil resources will be replaced in future, they won't be needed anymore for the generation of energy and renewable sources could become more important for the chemical industry as well. Wood is a source, which is already used very intensively in industry to produce paper and textiles, but not for production of bulk and fine chemicals. During the process of the production of paper byproducts are formed. One of these byproducts is acetic acid. In actual processes, acetic acid is incinerated among other byproducts as lignin [1]. Acetic acid is commonly used in food, pharmaceutical and plastics industry. In 2009 about 10 mt a^{-1} acetic acid dry were produced [2]. Thus, acetic acid represents a big market and the incineration is a big waste of money. In the paper industry acetic acid appears during the pulping of wood among other low molecular weight carboxylic acids in low concentrations, because of cleavage of the acetyl group from hemicelluloses [1]. A selective and effective process for isolating acetic acid needs to be developed. Low concentrations of some carboxylic acids can form azeotropic mixtures with water. Therefore, a thermal separation like distillation is not possible or not efficient [1]. Another possibility is extraction. Acetic acid should be transferred into another liquid, which is not miscible with water. This process can be enhanced by using a reactive extraction. In reactive extractions, the substance of interest is not only transferred into the other phase, also the effects of a chemical reaction can be used to increase the efficiency of recovery. Aliphatic amines and organophosphorous compounds as reactive reactants have been already reviewed [3]. These substances limit sustainability [4, 5] and operation range in reactive extraction due to their required residence time of up to 24h for efficient performance [6]. 1-octanol as alternative has already been investigated as reactive extractant. Recovery efficiency of acetic acid due to esterification could be enhanced by the addition of the surfactant 4-Dodecylbenzenesulfonic acid (DBSA) or sulfuric acid as catalyst [6]. The issue of using these catalysts, is their solubility in water [6]. During processing, catalyst gets lost into the aqueous phase, which would demand a purification process of the aqueous phase afterwards. This problem can be avoided by using membrane reaction technology, were DBSA is fixed [7]. However, interfacial area and thus reaction rate or physical extraction is limited in this technology. DBSA can by modified to a gemini surfactant formed by the reaction with $Ni(OH)_2$ to the water-insoluble metallosurfactant $NiDBSA_2$ [1]. A process concept, including regeneration of solvent and catalyst by reactive distillation is already developed [8]. This concept is composed by three steps. Reactive extraction of acetic acid from aqueous feed, phase separation and reactive distillation of loaded

solvent. During reactive extraction octyl acetate is formed (esterification) and dissolved in solvent. After separation of the phases, loaded solvent is treated with methanol in a reactive distillation (transesterification) for regeneration of the solvent 1-octanol, which is recycled to reactive extraction. In this task only the unit operation reactive extraction is considered. Fundamental understanding of the reactive extraction process regarding reaction and liquid-liquid equilibrium is needed to save chemicals, time and money. The fundamental understanding of this should be expressed by characteristic numbers like conversion and recovery and a mathematical model of the kinetics of the reactive extraction.

Research question

Is a monophasic kinetic model accurately applicable for the reactive extraction of acetic acid from diluted aqueous solutions based on experimental data?

Aims of the Thesis

This study is dedicated to answering the defined research question by investigating biphasic esterification of acetic acid in batch experiments. A synthetic feed of 1 mol L^{-1} acetic acid should be used together with a metallosurfactant catalyst for testing various kinetic models.

2 Theoretical Background

A reactive extraction is characterized by two main phenomena. The physical extraction of the substance of interest (solute) and the chemical reaction. The chemical reaction can enhance the recovery efficiency and optimize selectivity if multiple compound feeds are used.

2.1 Physical Extraction

In a physical extraction system at least two immiscible phases are used, and one or more solutes are transferred between the phases. The analyzed system is defined by two phases, the aqueous feed solution and the organic solvent (1-octanol). The solute is defined as acetic acid in this system. The transfer of solute is caused by its difference of solubility in both phases [9]. No chemical bonding between the solvent and solute appears in physical extraction. After reaching an equilibrium, the solute is distributed over both phases by a constant ratio. This ratio is defined as distribution coefficient K_D (Equation 1) [9].

$$K_{D,j} = \frac{c_{j_{org}}}{c_{j_{aqu}}} \tag{1}$$

K_D is defined as the ratio of the concentrations of the substance j in the immiscible organic and aqueous phases. Depending on the projected application, diluents can be added. These diluents must be mixable with or soluble in the solvent. They can have various effects on the solvent, not only K_D can be affected, also physical properties like viscosity, density, volatility can be altered [9]. In physical extraction, the mixing of both phases is crucial to enable an optimal transfer of the solute. The demand of energy for mixing increases with viscosity. Because of its lower viscosity than 1-octanol (7.288 mPa s, 25 °C), *n*-undecane (1.082 mPa s, 25 °C) was tested as diluent [10, 11].

2.2 Reactive extraction

Recovery efficiency and selectivity can be enhanced by combining a physical extraction with a chemical reaction. This hybrid method is called reactive extraction. The solvent or a substance dissolved in the solvent reacts with the solute in the feed phase. The product should be only soluble in the solvent phase.

2.3 Chemical reaction

In this investigation, reversible reaction of the solute acetic acid with the solvent 1-octanol was analyzed. Such reactions of carboxyl acids with alcohols are called esterification and are generally catalyzed by acidic catalysts (Figure 1) [1].

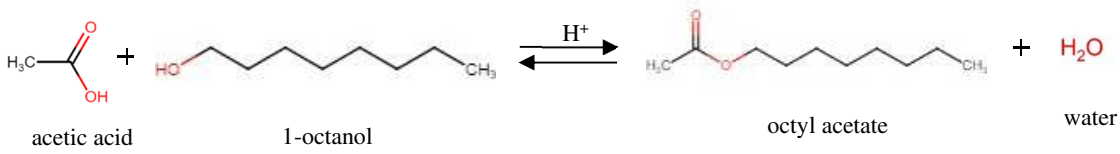

Figure 1: Chemical reaction of acetic acid and 1-octanol to octyl acetate and water catalyzed by acidic catalyst.

Since 1-octanol is the solvent and not miscible with water, the esterification occurs on the interface between aqueous and organic phases. Octyl acetate is also a highly unpolar molecule and thus only soluble in 1-octanol. Due to esterification and the physical extraction, acetic acid is pulled out of the aqueous phase and is enriched in 1-octanol as acetic acid itself or in form of octyl acetate. The reaction needs a minimum temperature and utilization of an acidic catalyst [1]. As already described in chapter 1, several catalysts like DBSA and sulfuric acid were analyzed in previous research and the water-insoluble metallosurfactant $NiDBSA_2$ appeared to be an alternative. $NiDBSA_2$ is produced by the reaction of DBSA and Nickel(II) hydroxide ($Ni(OH)_2$) (Figure 2) [1].

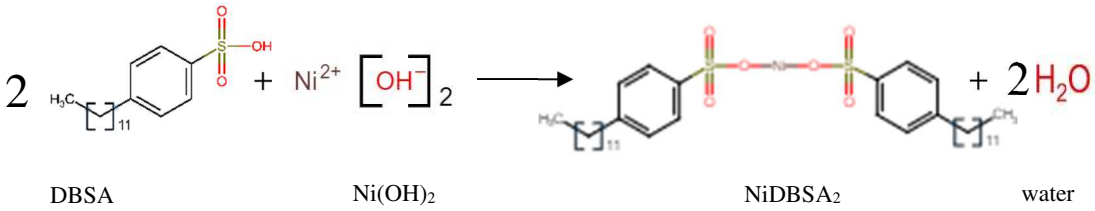

Figure 2: Chemical reaction of DBSA and $Ni(OH)_2$ to $NiDBSA_2$ and water

2.4 Surfactants

Due to their molecular shape of the hydrophilic head (red) and the hydrophobic tail, surfactants enrich at the interface of the two immiscible phases. Surfactant molecules form micelles if these phases get in touch (Figure 3) [12]. Micelles are closed three-dimensional formations, which can encapsulate the organic phase (hydrophobic) and are dispersed in the aqueous phase. If an aqueous phase is dispersed in an organic phase, reverse micelles are formed. This means the aqueous phase is encapsulated by the micelle and the hydrophilic heads are oriented to the inside

of the micelle and aqueous phase. The hydrophobic tails are oriented to the outside organic continuous phase (Figure 4).

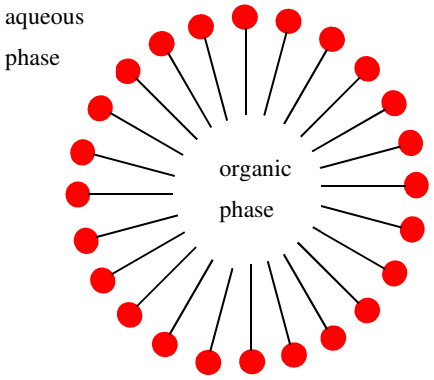

Figure 3: Sketch of a micelle; red circles define the hydrophilic heads and the black lines define the hydrophobic tails

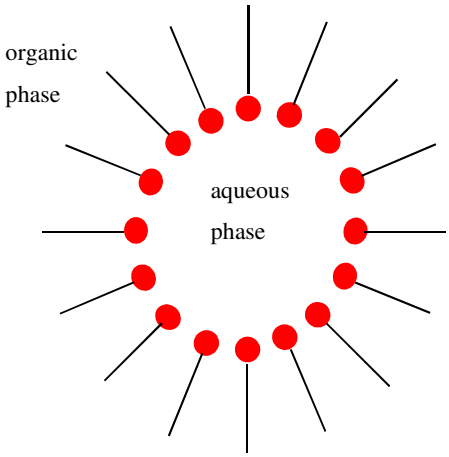

Figure 4: Sketch of a reverse micelle; red circles define the hydrophilic heads and the black lines define the hydrophobic tails

The shape of these formations is shown as a sphere in Figure 3 and Figure 4, exemplary. It does not need to be spherical necessarily. Bilayers, ellipsoids or vesicles are also known [13, 14], especially for systems with gemini surfactants. In this task, $NiDBSA_2$ was used as surfactant. Depending on molecule structure of a surfactant, predictions about its behavior in a biphasic system can be made, whether the surfactant forms micelles or reverse micelles. A useful concept is the Hydrophilic-Lipophilic Balance (HLB). This concept uses an empirical equation and functional groups present in molecules of commonly used surfactants. These functional groups refer to a certain value. A characteristic value for HLB can be calculated for each type of surfactant. The concept is not applicable on gemini surfactants like $NiDBSA_2$ but can be applied on DBSA. For DBSA, HLB number of 13-15 is determined [8]. Surfactants with HLB number greater than seven tend to form reverse micelles respectively water-in-oil emulsions [15]. One molecule of $NiDBSA_2$ is composed by two molecules of DBSA, thus the lipophilic part is doubled compared to DBSA. $NiDBSA_2$ is supposed to behave similar as DBSA or as a surfactant with even higher HLB number.

Another possibility for determining the preferred phase of a surfactant is the logP number [16]. logP is the logarithmic distribution coefficient of any substance in an octanol/water system and experimentally determined. Low logP means highly soluble in octanol. Predictions can be made that long alkyl chains lower the logP value. This is the case for DBSA and $NiDBSA_2$.

The ability to formation of micelles requires a minimum concentration of surfactant in the continuous phase. This concentration is called critical micelle concentration (CMC) [12]. CMC can be determined by measuring the surface tension at various concentrations of surfactant c_S (Figure 5) [17]. The scale of abscissa must be logarithmic to generate this kind of curve. CMC is defined as the intersection of the two linear regressions A of the values after the turning point and the slope B before [18].

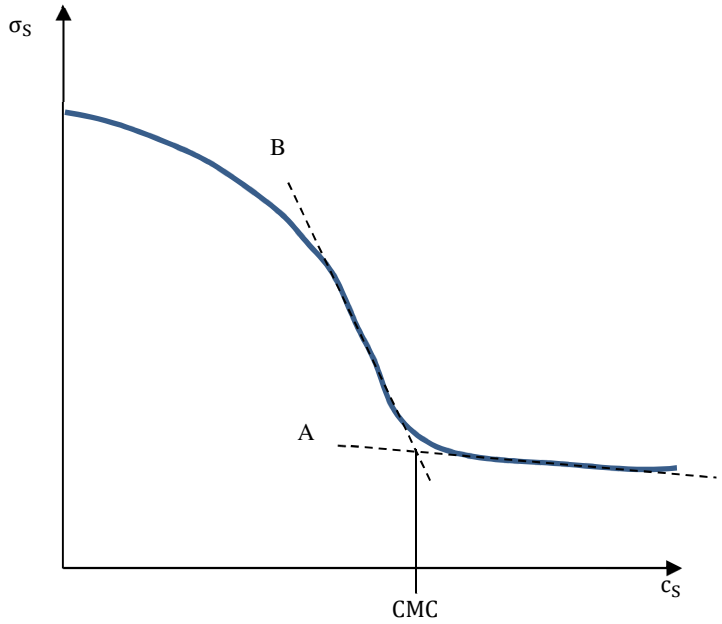

Figure 5: Determination of CMC by isotherm of surface tension

As seen in literature, the CMC can be very low, for example 5.51 10^{-4} mol L^{-1} DBSA in water [1]. The decrease of surface tension can be described by the Gibbs Adsorption Isotherm equation according to *Garrido* [15, 19].

If aqueous and organic phase are mixed together, they form emulsions. In emulsions, one phase is dispersed in the other. Depending on the concentration of catalyst and temperature, equilibrated emulsions show different behavior. High concentrations of catalyst (highly above CMC) can lead to thermodynamic stable microemulsions, which cannot be separated gravitationally [20]. This leads to a more complex overall process, as a sufficient phase separation step needs to be implemented.

$NiDBSA_2$ is a gemini surfactant with the hydrophilic head, the sulfonic acid-nickel-group and the two hydrophobic tails of the sulfonic acid. The advantage of $NiDBSA_2$ over other acids and surfactants tested is the insolubility in water and the prevention of emulsification, which enables good mixing and subsequent separation of the phases [1]. $NiDBSA_2$ is only dissolved in organic

phase and does not appear in the aqueous phase in significant concentrations. Therefore, the aqueous phase does not need to be purified. Another effect of surfactants in biphasic systems is the decrease of the interfacial tension between the phases [1]. This decrease is caused by adsorbed molecules of metallosurfactant at the interface, which form a film, weaken interfacial forces and enable mixing [21]. Hence, lower stiffness of the interface increases the ability of molecules to get transferred between phases [22].

2.5 Reaction kinetics

Surfactants at concentrations above CMC reduce the interfacial tension and form micelles, thus a quasi-monophasic system is assumed for modeling kinetics of the present reactive system. As seen in Figure 1, esterification is a reversible reaction. Such reactions are well researched and kinetic models do exist [23]. The reaction can be written schematically as seen in Equation 2.

$$aA + bB \underset{k_2}{\overset{k_1}{\rightleftharpoons}} rR + sS \tag{2}$$

A and B are the reactants, in this investigation acetic acid and 1-octanol. R and S are defined as products, octyl acetate and water. a, b, r and s are the stoichiometric factors of each compound in the reaction. As seen in the chemical reaction equation, they all equal to one (Figure 1). k_1 defines the reaction rate constant of the forward reaction and k_2 the one of backward reaction. Water is present by excess in the system because an aqueous solution of acetic acid was used as a feedphase. Thus, the concentration of water was assumed as constant and thus not considered explicitly in the kinetic models. The effect of water is included in the value of k_2. This consideration is also used for the concentration of 1-octanol in the organic phase and k_1. Further, distinction between stoichiometric feed and non-stoichiometric feed must be done. Stoichiometric feed means, the ratio of initial concentrations of reactants equals to the ratio of the stoichiometric factors of the reactants in the chemical reaction equation. For example a : b = $c_{A,0} : c_{B,0}$. In this task diluted aqueous solutions of acetic acid and undiluted 1-octanol with dissolved catalyst are used, which leads to non-stoichiometric feed. Additionally, constant volume is assumed during the reaction. Several parameters are used for describing the kinetic behavior (Equation 3, 4 and 5).

$$X_A = \frac{c_{A,0} - c_A}{c_{A,0}} \tag{3}$$

X_A defines the conversion, the ratio of the concentration of reacted compound A against its initial concentration. $X_{A,e}$ defines the conversion in equilibrium.

$$M_{BA} = \frac{c_{B,0}}{c_{A,0}} \tag{4}$$

$$M_{RA} = \frac{c_{R,0}}{c_{A,0}} = 0 \tag{5}$$

M_{BA} and M_{RA} define the ratio of the initial concentrations of B and R against the initial concentration of the limiting reactant A. The kinetic behavior of a reaction is not only defined by its reaction rate constant, but also by the order of each reactant. Several rate laws are investigated by *Ancheyta* [23]. Rate laws, those could possibly suit the investigated kinetic system, are tested (Equation 6, 7 and 8).

$$-r_{A,1} = -\frac{dc_A}{dt} = k_1 c_A c_B - k_2 c_R \tag{6}$$

$$-r_{A,2} = -\frac{dc_A}{dt} = k_1 c_A - k_2 {c_R}^2 \tag{7}$$

$$-r_{A,3} = -\frac{dc_A}{dt} = k_2 {c_A}^2 - k_1 c_R \tag{8}$$

Equation 6 defines a rate laws with both reactants (acetic acid and 1-octanol) contributing, while concentration of water is assumed as a constant because of its presence in excess. Equation 7 and 8 describe a rate law with only one reactant (acetic acid) contributing to the rate law, which means concentration of water and 1-octanol are considered to be present in excess. The integrated solutions of the rate laws depend on the parameters $c_{A,0}$, $X_{A,e}$, M_{BA} and M_{RA}, which are composed to the factors equilibrium constant K, f_a, f_b and f_c (Table 1). Depending on the type of reaction (number of contributing reactants) and the rate law (Equations 6, 7 and 8), definitions of these factors are different.

Table 1: Definitions of equilibrium constant K, f_a, f_b and f_c dedicated to their rate law

# of reactants	Rate law	K	f_a	f_b	f_c
1	$-r_{A,1}$	$\frac{M_{RA} + \frac{r}{a}X_{A,e}}{c_{A,0}(1 - X_{A,e})(M_{BA}\frac{b}{a} - X_{A,e})}$	$\frac{b}{a}c_{A,0}$	$-c_{A,0}\left(\frac{b}{a} + M_{RA}\right) - \frac{r}{aK}$	$c_{A,0}M_{BA} - \frac{M_{RA}}{K}$
2	$-r_{A,2}$	$\frac{c_{A,0}(M_{RA} + \frac{r}{a}X_{A,e})}{1 - X_{A,e}}$	$\frac{r^2 c_{A,0}}{a^2 K}$	$-1 - \frac{2rM_{RA}c_{A,0}}{aK}$	$1 - \frac{{M_{RA}}^2 c_{A,0}}{K}$
2	$-r_{A,3}$	$\frac{M_{RA} + \frac{r}{a}X_{A,e}}{c_{A,0}(1 - X_{A,e})^2}$	$c_{A,0}$	$-2c_{A,0} - \frac{r}{aK}$	$c_{A,0} - \frac{M_{RA}}{K}$

f_a, f_b and f_c are needed to determine the integrated form of the rate law by their criteria in the left column (Table 2). k_2 expressed as k_1/K in the derivation of the analytical solution of k_1.

Table 2: Integrated solution of rate law, rearranged to rate constant k_1 depending on f_a, f_b and f_c

Criterium	k_1	
${f_b}^2 > 4f_af_c$	$\frac{1}{D_1 t}\ln\frac{(2f_aX_A + f_b - D_1)(f_b + D_1)}{(2f_aX_A + f_b + D_1)(f_b - D_1)}$	$D_1 = \sqrt{{f_b}^2 - 4f_af_c}$
${f_b}^2 < 4f_af_c$	$\frac{1}{D_2 t}\left(\tan^{-1}\frac{2f_aX_A + f_b}{D_2} - \tan^{-1}\frac{f_b}{D_2}\right)$	$D_2 = \sqrt{4f_af_c - {f_b}^2}$
${f_b}^2 = 4f_af_c$	$\frac{1}{t}\frac{4f_aX_A}{f_b(2f_aX_A + f_b)}$	-

If X_A is measured over time, k_1 can be determined. Models with a constant behavior of k_1 fit the investigated reaction. If a constant k_1 is found, the dedicated equation can be rearranged to model X_A over time.

2.6 Order of Catalyst

The amount of catalyst is affecting the kinetic behavior of a chemical reaction. This impact can be described by the introduction of an order of catalyst according to *Burés* [24, 25]. The graphical method uses a time-normalized abscissa and the concentration of the product as ordinate. The method is shown exemplary for two different concentration of catalyst c_{cat} (Figure 6 and Figure 7).

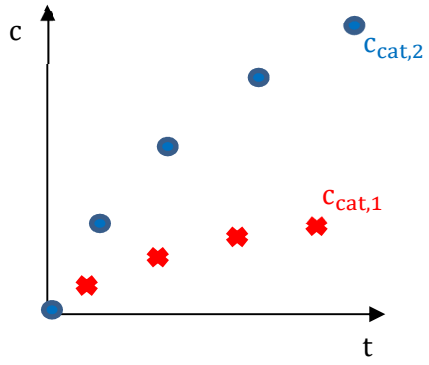

Figure 6: Application of Burés Time Normalization Method; Product concentration over time and $c_{cat,1} < c_{cat,2}$

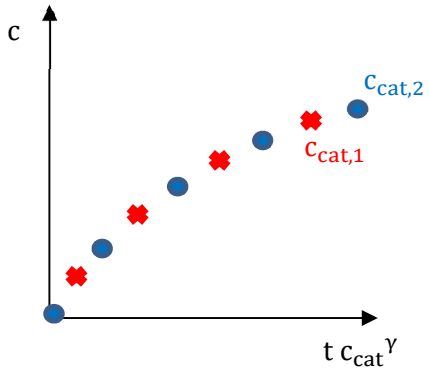

Figure 7: Application of Burés Time Normalization Method; Product concentration over time with γ as order of catalyst and $c_{cat,1} < c_{cat,2}$

Exponent γ in the term $t\, c_{cat}^{\gamma}$ is varied until both curves match each other. The determined value for γ is defined as the order of catalyst. The method has not been applied on biphasic system yet but is considered as a possibility to describe the effect of catalyst on reaction kinetics.

3 Experimental procedure

The investigated system is generally characterized by an extraction and chemical reaction process. In this task, the two main processes were analyzed separately. First, experiments on the extraction process, meaning liquid-liquid-equilibrium (LLE) of acetic acid and co-extraction of water are described. Data of these experiments is used for screening optimal composition of solvent phase, to determine distribution coefficients. Secondly the experiments on reaction kinetics for determination of a valid kinetic model and dedicated rate constants, equilibrium constants, conversion and recovery efficiency. Measurements of the surface and interfacial tensions are described afterwards. In all experiments, $NiDBSA_2$ was used as catalyst. This surfactant has a major impact on the processes of extraction and reaction, mainly because of its effects on the interface between the phase. Former defined solutions must be used for both phases. These solutions are defined for each experiment in the dedicated experimental plans.

3.1 Materials

All technical equipment and chemical resources used in experiments are described in the following section.

3.1.1 Experimental devices

Several devices were used for different experiments. In Table 3, all devices are dedicated to their related experiment.

Table 3: Experimental devices with type and company, dedicated to related experiments (LLE, kinetics, surface tension, interfacial tension)

Type of experiment	Device	Type and company
Liquid-liquid-equilibrium (LLE)	Shaker	HS500 from Janke & Kunkel
	Thermostat	LAUDA ecoline RE206 from LAUDA
	Centrifuge	EBA 8 from Hettich
Kinetics	Thermostat	LAUDA ecoline RE104 from LAUDA
	Heating and stirring	Heidolph MR Hei-Standard from heidolph
	Centrifuge	EBA 8 from Hettich
	Shaking water bath	GFL 1083 from GFL
Surface tension	Tensiometer	TVT 2 from LAUDA
Interfacial tension	Thermostat	Julabo 200F from Julabo
	Refractometer	PAL-RI from ATAGO
	Tensiometer	SVT 20 from dataphysics; Method: Laplace-Young method (LY)

3.1.2 Analysis

Samples generated by experiments were analyzed on composition and density. Concentrations of acetic acid, 1-octanol and octyl acetate in both phases were analyzed in a Shimadzu GC2010plus equipped with a flame ionization detector (FID). A Zebron ZB WAXplus column with 60 m length, 0.32 mm inner diameter and a film thickness of 0.5 µm was used. The gas chromatograph was operated in split mode (split ratio 120) with helium as carrier gas. Injection of 0.3 µL of sample via AOC 20i/s autosampler was done at 250 °C; the detectors were operated at 270 °C. The oven program started with a hold at 40 °C for 6.5 min and a temperature plateau at 60 °C for 2.5 min. This was followed by another temperature plateau at 120 °C held for 2 min and a final increase to 200 °C without hold time. The heating rate in-between the temperature plateaus was 20 °C min^{-1}. Samples were precooled to 5 °C in the autosampler and injected undiluted. Mass fraction of water in the organic phase was measured by the Karl-Fischer-titration using the titrator SI Analytics Titrator Titroline 7500 from xylem. Density of both phases was measured by the densimeter SVM 3000 from Anton Paar.

3.1.3 Materials

4-dodecylbenzenesulfonic acid (>95%, mixture of isomers, Sigma-Aldrich), nickel(II) hydroxide ($Ni(OH)_2$, Sigma-Aldrich), *n*-undecane (>99%, Sigma-Aldrich), 1-octanol (>99%, Sigma-Aldrich) and acetic acid (>99%, ChemLab) were used as supplied without further purification.

3.2 Preparation of metallosurfactant catalyst

As catalyst the metallosurfactant $NiDBSA_2$ was used. This catalyst was developed by *Toth et al.*[1] and was produced by the reaction of 4-dodecylbenzenesulfonic acid (DBSA) and nickel(II) hydroxide ($Ni(OH)_2$). Both substances were weight in stoichiometric ratio of nickel to DBSA of 1 : 2. Afterwards, both substances are brayed in a mortar for 20 minutes and the product was dried in the mortar for three days at ambient temperature. The dried catalyst is dissolved in 1-octanol and rinsed with water, to wash out nonreacted DBSA or $Ni(OH)_2$ and counteract co-extraction of water (section 4.1.2) The maximal solubility of catalyst in 1-octanol was 28 wt%.

3.3 Liquid-liquid-extraction

The experiments on LLE were performed by using the shaker HS500 from Janke & Kunkel (Figure 8).

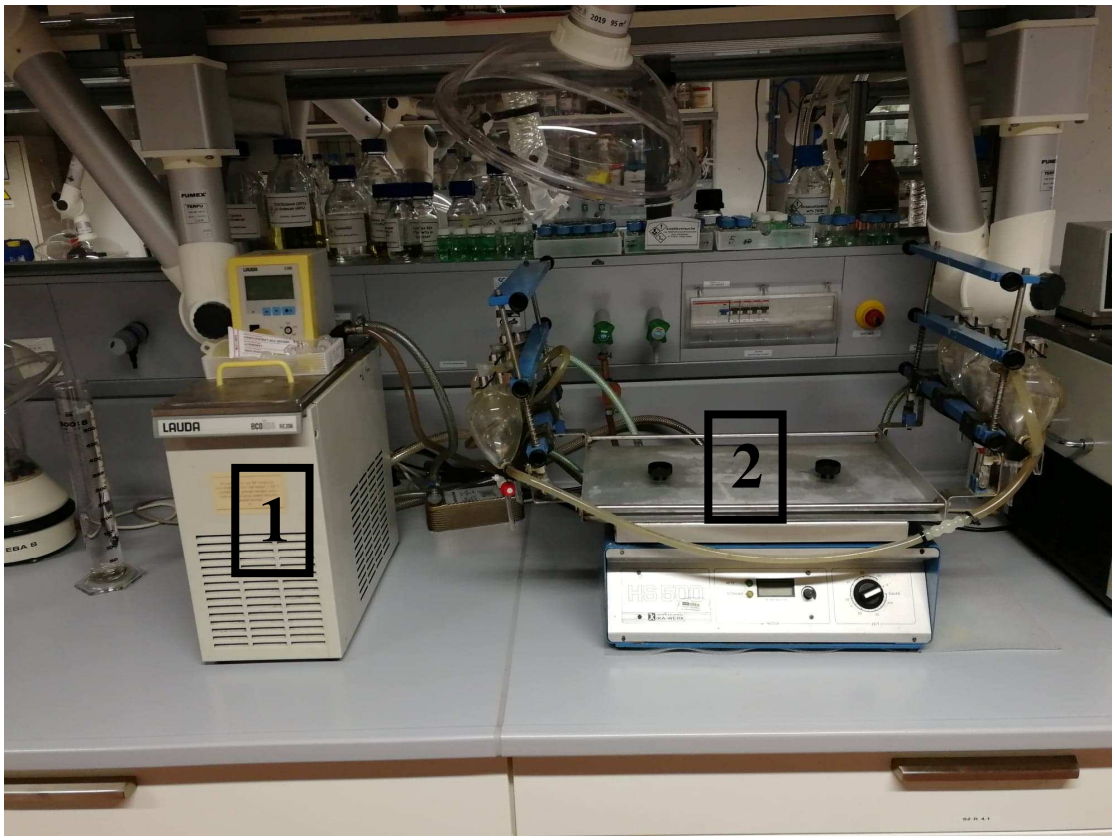

Figure 8: Apparatus for LLE experiments with thermostat (1) and shaker (2)

A constant temperature during all experiments was enabled by the thermostat. Table 4 summarizes the experimental parameters, which were the same for all LLE experiments.

Table 4: General settings of Experiments on LLE

Volume ratio of phases	1
Volume of each phase	7 mL
Shaking speed	180 strokes per minute
Time of shaking	30 min
Time of relaxation	10 min

The device has six separating funnels. Thus, six experiments could be done simultaneously at the same temperature. Both phases were filled in the separating funnels of the shaker, funnels were closed, and the shaker was started. After 30 minutes of shaking, the shaker was stopped and rested 10 minutes for relaxation to enable phase separation. In case phase separation was not reached in this time (especially at higher mass fractions of catalyst and lower temperatures), the sample was centrifuged, and the phases were separated afterwards. About 1 mL of each separated phase was filled in a GC-Vial for analyzing the containments (acetic acid, octyl acetate, 1-octanol). The content of water in the organic phase was determined by Karl Fischer titration (KF) as a triple determination for each sample. The density of each sample was

measured by densimeter. All experiments were done twice as double determination. This procedure was used to execute three different sets of LLE experiments. The first was used to screen the effects of solvent composition in dependence of the extraction temperature. The second set was designated to investigate the impact of the load of metallosurfactant catalyst on distribution coefficents. In the third set the change in the LLE's due to initially present octyl acetate was investigated. These three sets are described in the following subchapters.

3.3.1 Screening for optimal composition of solvent

The first experiments were about to find the optimal mix of substances of the organic phase containing 1-octanol as solvent and *n*-undecane as diluent. No surfactant was used in these experiments. Mixtures of 1-octanol and *n*-undecane were tested at several ratios of mass fractions ($\mathrm{rat_{Oct/Und}}$) with aqueous phases with initial concentrations ($\mathrm{c_{HAc_{aqu,0}}}$) from 1 to 100 g L^{-1} acetic acid were used (Table 5). All experiments were done at the temperature of 25 °C.

Table 5: Experimental plan for the screening for optimal solvent composition (mixtures of 1-octnaol and n-undecane) for acetic acid extraction

organic phase	Initial acetic acid concentration $c_{HAc_{aqu,0}}$[mol L^{-1}] ($g\ L^{-1}$)			
1-octanol undiluted	0.0167 (1.00)	0.100 (6.00)	1.00 (60.00)	1.670 (100.00)
1-octanol/undecane $rat_{Oct/Und} = 70/30$ wt%	0.0167 (1.00)	0.100 (6.00)	1.00 (60.00)	1.670 (100.00)
1-octanol/undecane $rat_{Oct/Und} = 50/50$ wt%	0.0167 (1.00)	0.100 (6.00)	1.00 (60.00)	1.670 (100.00)

3.3.2 Experiments for determination of molar loads and distribution coefficients

As the optimal solvent, undiluted 1-octanol was determined (section 4.1.1). Organic phases used in these experiments contained the catalyst $NiDBSA_2$. Mass fraction of catalyst was varied. Each mass fraction was tested with aqueous phases of initial concentrations from 1 to 200 gL^{-1} acetic acid. These experiments were also done at different temperatures (25, 40, 60 °C). The following combination of solutions were used (Table 6)

Table 6: Experimental plan for the experiments for determination of molar loads and distribution coefficients in dependence of temperature and catalyst load

Initial organic phase	Initial acetic acid concentration $c_{HAc_{aqu,0}}$ [mol L^{-1}] ($g\ L^{-1}$)				
$NiDBSA_2$ in 1-octanol $w_{cat} = 5$ wt%	0.0167 (1.00)	0.100 (6.00)	1.00 (60.00)	1.670 (100.00)	3.330 (200)
$NiDBSA_2$ in 1-octanol $w_{cat} = 20$ wt%	0.0167 (1.00)	0.100 (6.00)	1.00 (60.00)	1.670 (100.00)	3.330 (200.00)

3.3.3 Experiments for determination of the distribution coefficient with initial octyl acetate

To analyze the influence of the octyl acetate on the equilibrium of physical extraction, a series of experiments was done with initial octyl acetate in organic phases. Therefore, octyl acetate was added to already existing solutions of $NiDBSA_2$ in 1-octanol at the ratio of $n_{Oct} : n_{OctAc}$ of $10 : 1$. The mass of added octyl acetate is defined in Equation 9.

$$m_{OctAc,add} = \frac{m_{org}\,(1 - w_{cat} - w_W)}{M_{Oct} * 10} M_{OctAc} \tag{9}$$

The following combinations of solutions were used and summarized in Table 7.

Table 7: Experimental plan for experiments for distribution coefficient with initial octyl acetate (defined in Equation 9)

Initial organic phase	Initial aqueous phase with $c_{HAc_{aqu,0}}$ [mol L^{-1}] ($g\ L^{-1}$)			
$NiDBSA_2$ in 1-octanol $w_{cat} = 5\%$ + octyl acetate added	0.0167 (1.00)	0.100 (6.00)	1.00 (60.00)	1.670 (100.00)
$NiDBSA_2$ in 1-octanol $w_{cat} = 20\%$ + octyl acetate added	0.0167 (1.00)	0.100 (6.00)	1.00 (60.00)	1.670 (100.00)

3.4 Reaction kinetics

The reaction kinetics were investigated in a lab scale batch setup. This experimental setup is shown in the picture in Figure 9.

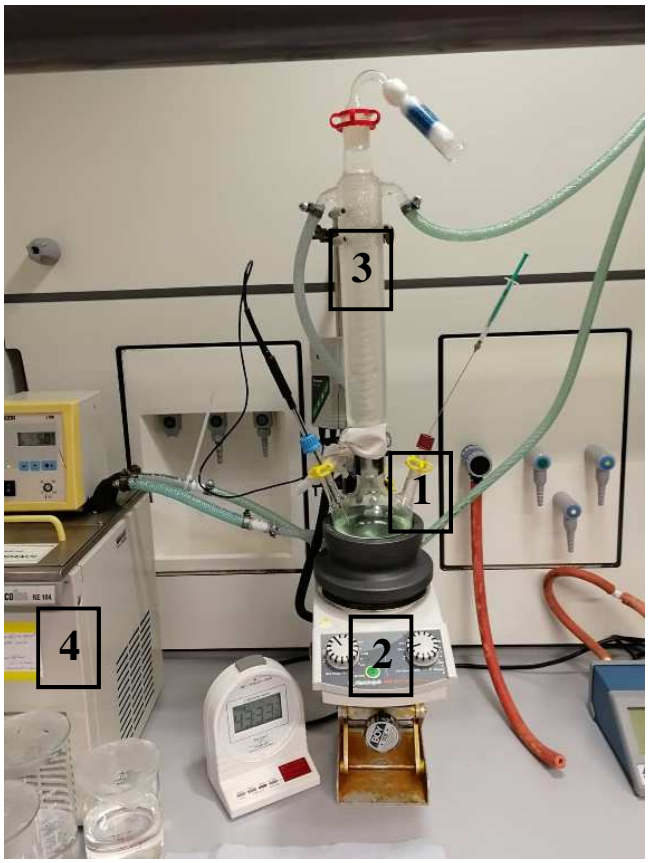

Figure 9: Experimental setup for kinetic batch experiments in lab scale for kinetic experiments with round-bottom flask (1), heating stirrer (2), cooler (3) and thermostat (4)

Both phases were mixed in the round bottom flask with three inlets (Figure 9, 1). Inside the round-bottom flask a magnetic stirrer was placed to enable a good mixing of the two phases during the experiment. The mixing was enabled by the heating and stirring device underneath of the round bottom flask (Figure 9, 2). A constant temperature was ensured also by this device in combination with temperature sensor in the left inlet of the round bottom flask. On the right, a syringe is used to add the acetic acid for starting the experiment. On the central inlet of the round-bottom flask, a cooler is used to ensure condensation reflux of any solvent (Figure 9, 3), water or acetic acid. Additionally, the cooler is closed by a silica gel (blue) at the top to avoid transfer of water vapor in or out. The temperature of the cooler was held constantly at 5 °C by the thermostat on the left of Figure 9 (4). All connections of the round-bottom flask to the cooler, syringe and thermometer had to be tight. Important constant parameters in these experiments are listed in Table 8.

Table 8: General settings of experiments on reaction kinetics

Stirrer speed	285-290 min^{-1}
Volume ratio of organic and aqueous phases	1
$V_{org,0}$	150 mL
$V_{aqu,0}$	150 mL
$c_{HAc,aqu,0}$	1 mol L^{-1} (60 g L^{-1})
Temperature of cooler	5 °C

The stirrer speed was limited. At higher speed, the stirrer tended to lose stable position in the bottom of the flask and started to bounce. At the beginning the organic phase and a certain amount of water were filled in together in the round-bottom flask. The certain amount of water is estimated by the following assumption, that acetic acid and water together form an ideal mixture (Equation 10).

$$c_{HAc_{aqu,0}} = \frac{m_{HAc}}{V_{aqu,0}} = \frac{\frac{m_{HAc}}{M_{HAc}}}{\frac{m_{HAc}}{\rho_{HAc}} + \frac{m_W}{\rho_W}} \quad (10)$$

Knowing the desired concentration of acetic acid and the volume of the solution, the needed amount of acetic acid and water can be calculated. The dependency on temperature of the densities was neglected in this calculation and densities at 25 °C were used for all substances. For 150 mL aqueous phase 141.10 g water and 9.09 g acetic acid were needed, this would lead to a 60 g L^{-1} solution. The calculated amount of water and the organic phase are mixed together in the round-bottom flask and the heating system was started. As soon as the desired temperature was reached, the whole amount of acetic acid was quickly added by the syringe. This splitting of the initial aqueous phase in acetic acid and water was necessary, to ensure, reaction was starting at the desired temperature only. By adding acetic acid, reaction was started, and samples were taken every 30 minutes by another syringe. The weights of samples were needed later for an estimation of the change in volume over time. Three minutes previously of taking the sample, the stirrer was stopped to ensure separation of phases. Samples of 1 mL were taken from each of the phases. The compositions of these samples were measured by GC and Karl Fischer titration. Three minutes of relaxation were not used in experiments at 25 °C and 20 wt% catalyst because phases did not separate in this time. 1 mL of mixed phases was used as sample, centrifuged and phases separated with a syringe. The composition of separated phases was measured by GC and KF. Each experiment was done over a period of five hours which resulted in ten samples per phase.

After five hours and the last sample, the round-bottom flask with its content was weight and transferred into a separation funnel to determine the mass of each phase after separation. The

densities of the separated phases were measured by densimeter and water content was measured by KF as triple determination. This whole procedure was done at various mass fractions of catalyst and temperatures according to Table 9. The initial concentration of acetic acid in the aqueous phase was fixed for all kinetic experiments with 1 mol L^{-1} (60 g L^{-1}) (Equation 10).

Table 9: Experimental plan of experiments on reaction kinetics

Temperature [°C]	Initial organic phase	Initial aqueous phase with $c_{HAc_{aqu,0}}$ [mol L^{-1}] (gL^{-1})
25	$NiDBSA_2$ in 1-octanol $w_{cat} = 5$ wt%	1.00 (60.00)
	$NiDBSA_2$ in 1-octanol $w_{cat} = 20\%$	1.00 (60.00)
40	$NiDBSA_2$ in 1-octanol $w_{cat} = 5$ wt%	1.00 (60.00)
	$NiDBSA_2$ in 1-octanol $w_{cat} = 20$ wt%	1.00 (60.00)
60	$NiDBSA_2$ in 1-octanol $w_{cat} = 5$ wt%	1.00 (60.00)
	$NiDBSA_2$ in 1-octanol $w_{cat} = 20$ wt%	1.00 (60.00)

Double determination was done by varying the time of taking the first sample. This means the time of taking the first sample in the first experiment was after 30 minutes and in the second one 15 minutes, but the interval of 30 minutes between taking the samples was kept constant for both experiments. These two curves should fit in each other (section 4.2).

Esterification is a reversible reaction, thus conversion in equilibrium must be determined for subsequent model development. This was done by experiments using shaking water bath. 0.5 mL of each initial phase were put in GC-vail and two of them were encapsulated in a closable testing tube padded with aluminium foil to avoid damages. These samples were shaken in water bath at constant temperature. In intervals of 24 hours in three days, the two phases in the samples were separated, and their composition analyzed by GC and KF. Density could not be measured because of the little volumes of the samples. Equilibrium conversion was determined for all combinations of temperature and mass fractions of catalyst listed in Table 9.

3.5 Measurement of surface tension

Critical micelle concentration CMC can be determined by measuring the surface tension of a solution containing surfactants. Surface tension was measured by the tensiometer. For this analysis, density of the solution is needed, which was measured by the densimeter. The tensiometer measures by drop volume method. For estimation of the critical micelle concentration samples of various concentrations of $NiDBSA_2$ in 1-octanol were used and their surface tension measured. Measurements were done at 25 °C.

3.6 Measurement of interfacial tension

The dynamic interfacial tension can be measured by the spinning drop video tensiometer. For estimation of the dynamic interfacial tension using this device, density of both phases, refraction index of the continuous phase and rotational speed are needed. Densities are measured by densimeter and refraction index is measured by the pocket refractometer. The spinning drop video tensiometer uses the spinning drop method. In this method the capillary was filled with the continuous phase (high density) and a droplet of the dispersed phase (low density) was added. Afterwards a rotational speed was applied on the capillary. The continuous phase is transferred to the outside of the capillary and the dispersed phase is transferred into the middle and forms droplets. Measuring size and shape of these droplets and knowing density of both phases, refraction index of the continuous phase and using the rotational speed, interfacial tension can be computed by the software using the Laplace-Young method. In this task, firstly separated phases from LLE-experiments were used as continuous phase (aqueous phase) and dispersed phase (organic phase). Using these solutions, no interfacial tension could be measured because non-reacted DBSA (section 3.2) was transferred from organic phase into the aqueous phase and formed foam in the middle of the spinning capillary. This foam can be seen in Figure 10 as gray stripe between and beside of the droplets (elliptic marks). The software cannot recognize the droplets in the video anymore and an interfacial tension cannot be measured. Thus, pure water was used as continuous phase. As seen in Figure 11, no gray stripe and no foam appeared anymore, and an interfacial tension could be measured. Like in measurements on surface tension, interfacial tension at various concentrations of $NiDBSA_2$ were measured as double determination.

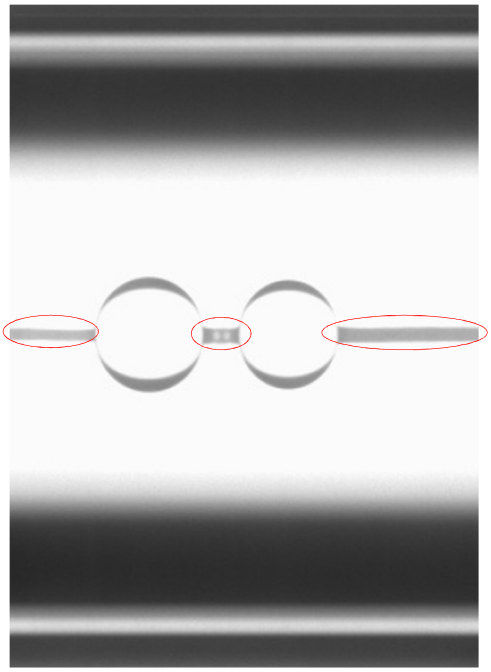

Figure 10: Measurement of interfacial tension (25 °C); phases in equilibrium after LLE experiments are used; continuous phase: aqueous phase with residual acetic acid and DBSA; dispersed phase: 1-octanol with transferred acetic acid, water and dissolved $NiDBSA_2$; foam caused by DBSA between and beside droplets (elliptic marks)

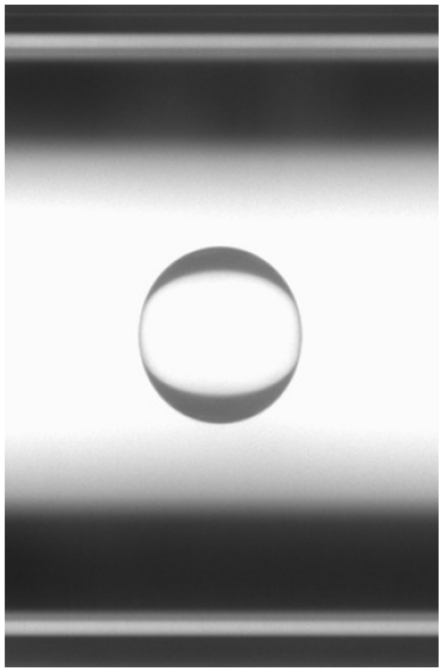

Figure 11: Measurement of interfacial tension (25 °C); continuous phase: pure water; dispersed phase: 1-octanol, transferred acetic acid, water and dissolved $NiDBSA_2$; (equilibrium of LLE experiment)

4 Results

This chapter summarizes the results of experiments on LLE, kinetics, surface tension and interfacial tension. Characteristic numbers like distribution coefficients, conversion, recovery, reaction rate constants or equilibrium constants are used to graphically represent and interpret the results.

4.1 Analysis of experimental data from LLE

The reaction superposing the extraction was not considered in primary evaluation of the experiments on LLE. This decision is based on the fact that little progress of the reaction occurs during the 30 minutes of extraction. This assumption could be confirmed by kinetic experiments as shown in section 4.2, Figure 21. Acetic acid transferred in the organic phase in equilibrium is defined as the sum of the concentrations of acetic acid and octyl acetate (Equation 11).

$$c_{HAc,org,tr} = c_{HAc,org} + c_{OctAc} \tag{11}$$

All experiments were done as double determination. The points in the diagrams are defined as the averages of the two measured results. The standard deviation due to the double determination is shown in diagrams as errorbars.

4.1.1 Determination of optimal composition of solvent

The recovery efficiency of acetic acid from the aqueous phase is the crucial factor for determination of optimal ratio of mass fractions of 1-octanol and *n*-undecane ($rat_{Oct/Und}$). The experimental distribution of the acetic acid between both phases is shown in Figure 12.

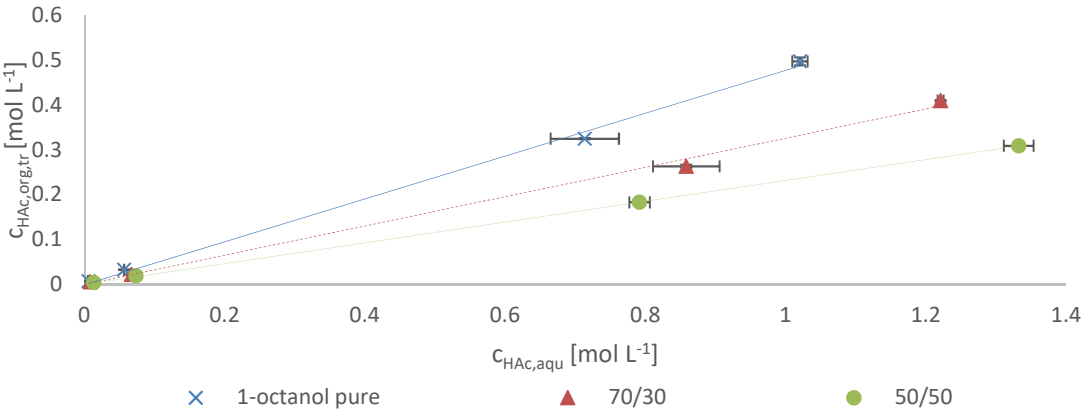

Figure 12: LLE of acetic acid; organic phase composed by various mixtures of 1-octanol and *n*-undecane; $rat_{oct/und}$= undiluted 1-octanol, 70/30, 50/50 (ratio of wt%); 25 °C; no catalyst; standard deviation is shown by errorbars

Distribution of acetic acid behaves linear over all analyzed initial concentrations for all analyzed mixtures of the organic phases. This is characteristical for physical extraction and confirms, saturation of the solvent phase with dissolved acetic acid does not occur in the analyzed range of acetic acid feed concentrations (0,0167 to 1,670 mol L^{-1}). Undiluted 1-octanol recovers acetic acid most efficiently from aqueous phase over the whole range of analyzed initial concentrations with a distribution coefficient of 0.48 compared to 0.33 (70/30 mixture) and 0.23 (50/50 mixture). *n*-undecane in the organic phase decreases efficiency of recovery. The double determination shows significantly divergence at the second highest points of the curves of $rat_{Oct/Und} = 70/30$ and undiluted 1-octanol. These points were measured after using an initial concentration of 1 mol L^{-1} acetic acid. These divergences should have random causes because the mean of the linear regression fits the mean of these points. Minor reaction of 1-octanol and acetic acid does also occur in these experiments (below 0.04 mol L^{-1} octyl acetate in organic phase). As shown in Figure 21, the reaction rate at 25 °C is very low, especially without catalyst. Thus, the reaction can be neglected in this analysis. The most efficient organic phase is the undiluted 1-octanol, which is used for the further experiments with catalyst. Water content of each sample measured by the KF titration are compared in Figure 13.

The diagram in Figure 13 correlates the water content of the equilibrated solvent samples with the initial acetic acid concentration for different solvent mixtures.

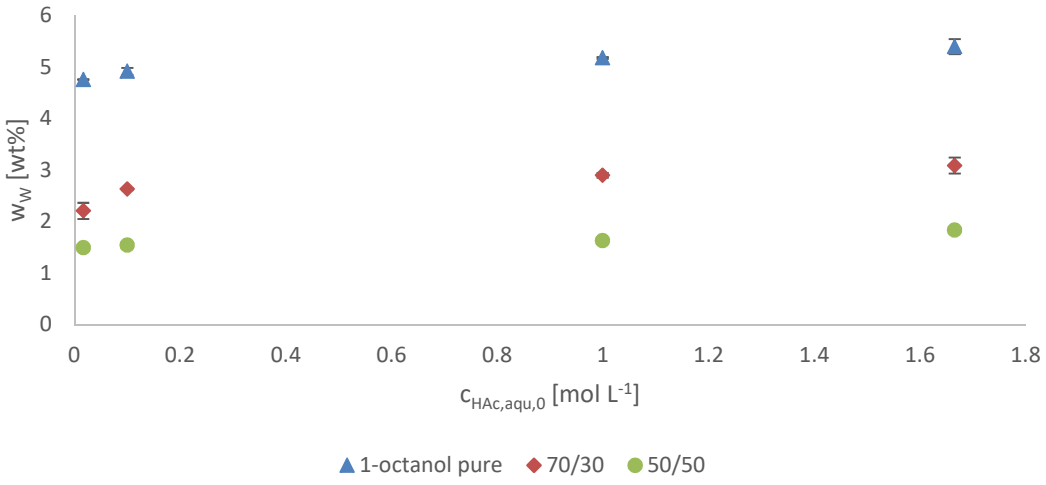

Figure 13: Influence of solvent composition (ratio of wt%) and initial acetic acid concentration on water content of solvent samples in equilibrium; organic phase composed by various mixtures of 1-octanol and *n*-undecane; $rat_{oct/und}$= undiluted 1-octanol, 70/30, 50/50 (ratio of wt%); 25 °C; no catalyst; standard deviation is shown by errorbars

The x-axis is defined as the initial aqueous concentration of acetic acid, used in each experiment. Generally, water content of organic phase increases slightly by increasing initial concentration of acetic acid. This could be because transferred acetic acid leads to a solvent with higher total polarity. Water can be dissolved better in solvents with higher polarity. Adding *n*-undecane to

1-octanol reduces mass fraction of water because of *n*-undecane is not a polar solvent and thus the solubility of acetic acid also decreases. A 50/50 mixture of 1-octanol and *n*-undecane contains only about a fourth of the water compared to undiluted 1-octanol. Extraction efficiency of acetic acid was the main criterion for solvent selection. Higher co-extraction of water with undiluted 1-octanol was counteracted by saturating the solvent phase with water prior to the respective kinetic experiments (section 3.2). Co-extraction of water is generally a well-known phenomenon in reactive extraction of low molecular carboxylic acids [26].

4.1.2 Determination of molar loads and distribution coefficient of acetic acid

The influence of the metallosurfactant catalyst $NiDBSA_2$ on LLE was determined for catalyst loads of 5 and 20 wt%. These mass fractions are also analyzed at various temperatures (25, 40, 60 °C). A high catalyst load of 20 wt% also means, less solvent/reactant (1-octanol) is present in the organic phase. To illustrate the effect of the catalyst on the LLE of acetic acid, the molar load of acetic acid is compared. Molar load is defined as the ratio of the concentration of acetic acid as formerly defined in Equation 11 in numerator and the sum of the concentration of 1-octanol and octyl acetate in the denominator. This definition (Equation 12) was chosen because a minor amount of 1-octanol reacted during the experiment (see further: section 4.2).

$$L_{HAc} = \frac{c_{HAc,org,tr}}{c_{Oct} + c_{OctAc}} \tag{12}$$

At 25 °C very little reaction appeared (according to Figure 21), thus the error induced by the superposing reaction is minimum. Molar load related to initial aqueous concentration is shown exemplary in Figure 14 at both mass fractions of catalyst 5 and 20 wt%.

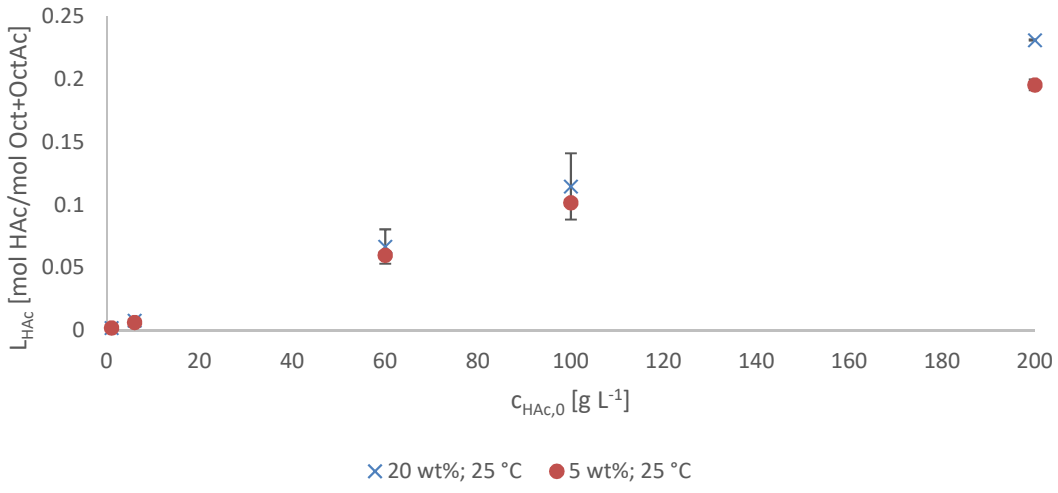

Figure 14: Comparison of molar loads of acetic acid in 1-octanol at 25 °C with 5 and 20 wt% of catalyst; related to initial aqueous concentration of acetic acid

According to Figure 14, the behavior of molar load stays linear in the whole analyzed range of initial concentration of acetic acid. Huge errors at 100 g L^{-1} and 60 g L^{-1} appear. This error is caused by high deviations of the concentration of 1-octanol measured by GC, which is the dominating value in the denominator in Equation 12.

From Figure 14 can be concluded that high mass fraction of catalyst enhances molar load of extracted acetic acid. Molar load could be increased by 20 %, comparing the numbers at 200 g L^{-1} acetic acid in the feed. The trend of increased efficiency is seemingly depending on the total acid amount present in the system. Further investigations are necessary to confirm this trend.

Molar load diagrams at 40 °C and 60 °C show similar behavior and can be found in Appendix A. The increase of the molar load by approximately 20 % at the higher mass fraction of catalyst can also be found at these temperatures. High errors in double determination are also caused by high variances of concentrations of 1-octanol.

The distribution coefficient of acetic acid is defined as the slope of the linear regression generated by data of equilibria concentration of acetic acid in organic phase related to the one in aqueous phase. This method is shown exemplary for 25 °C and 5 wt% catalyst (Figure 15).

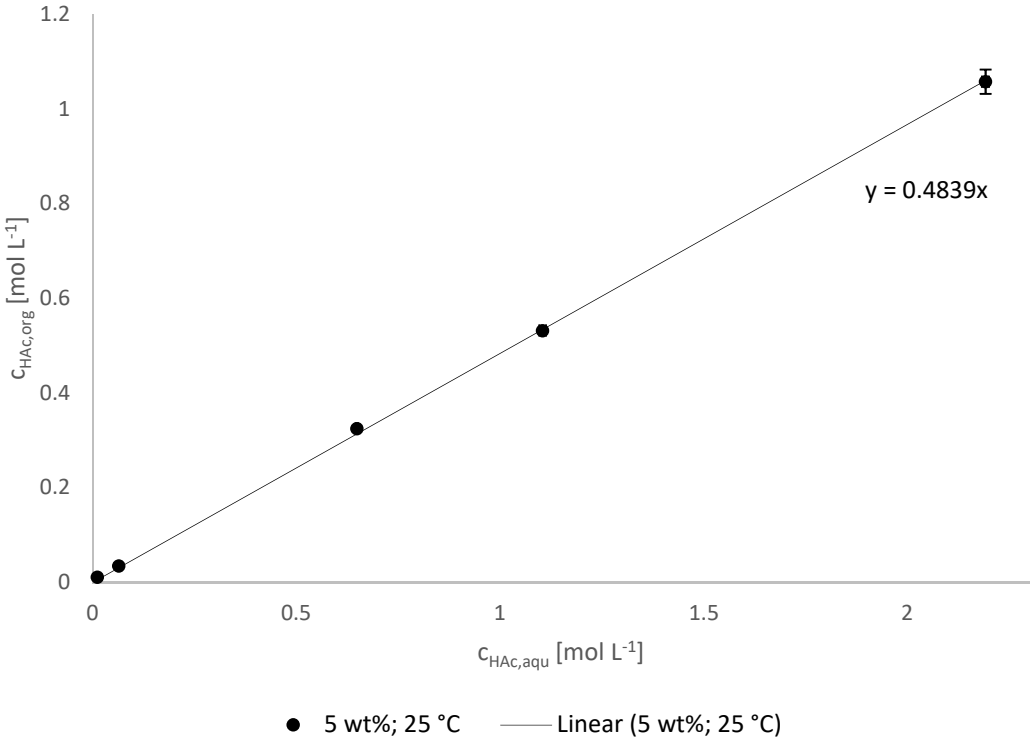

Figure 15: Determination of the distribution coefficient as slope in linear regression; 25 °C and 5 wt% catalyst

Distribution of acetic acid behaves linear in the analyzed range of concentrations (from 0.0167 to 1.670 mol L^{-1}). The linear equation generated by the linear regression is used for determining the distribution coefficient. In this case 0.48 can be defined as distribution coefficient K_D at 25 °C and 5 wt% of catalyst. This method is applied for every other combination of temperature and mass fraction of catalyst (Figure 16).

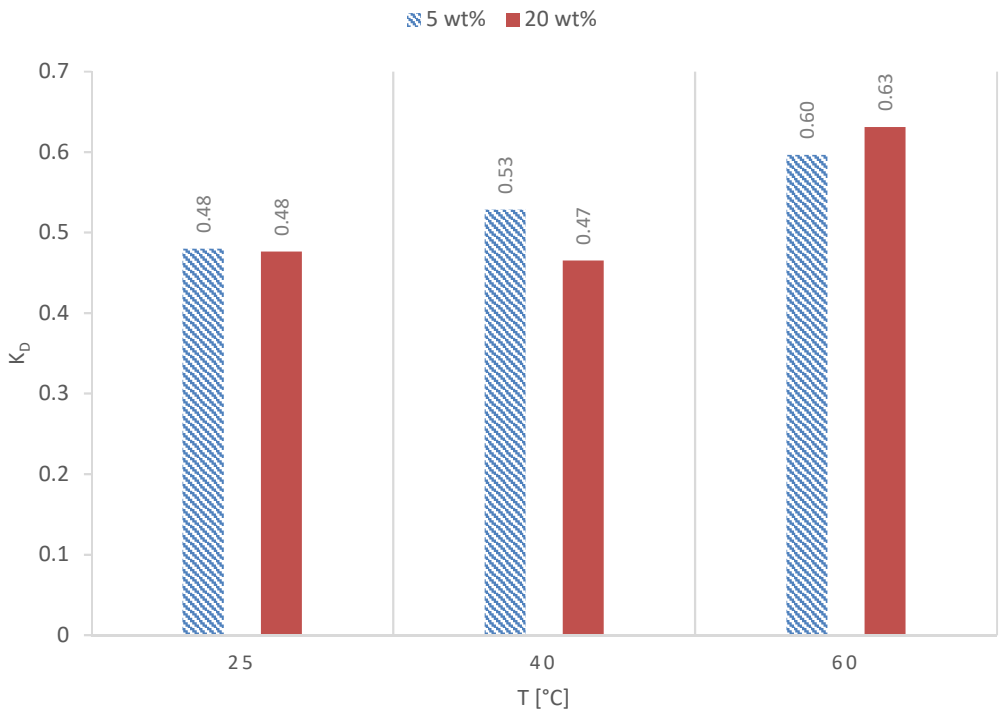

Figure 16: Comparison of distribution coefficients K_D at all analyzed combinations of temperature and mass fraction of catalyst

Distribution coefficients of 5 and 20 wt% are in a narrow range (0.48 - 0.63) at all temperatures but increase with temperature. Since 0.48 is also the distribution coefficient of acetic acid in a system without catalyst (section 3.3.1), no correlation of distribution coefficient with mass fraction of catalyst can be found. At 40 °C the higher distribution coefficient was found at 5 wt% catalyst, the opposite was found at 60 °C. A possible reason would be, that solvents with 5 wt% catalyst contain more 1-octanol, where more acetic acid is soluble (Figure 14). Error due to superposing esterification is higher at 60 °C. Because of the definition in Equation 11, the concentrations of octyl acetate and acetic acid are summarized. Esterification is enhanced by elevated temperature and more octyl acetate is formed. This leads to higher distribution coefficients.

Distribution coefficients of 1-octanol and octyl acetate could not be determined because their concentrations in the aqueous phase were below the measurable limit at all analyzed

temperatures. Insolubility of octyl acetate and 1-octanol is essential to enable efficient recovery performance of acetic acid and preventing subsequent purification of the aqueous phase.

Figure 17 shows the mass fraction of water (w_W) of the organic phase in equilibrium with respect to initial concentration of acetic acid. Only the results with a mass fraction of catalyst of 5% but all temperatures (25, 40, 60 °C) are shown.

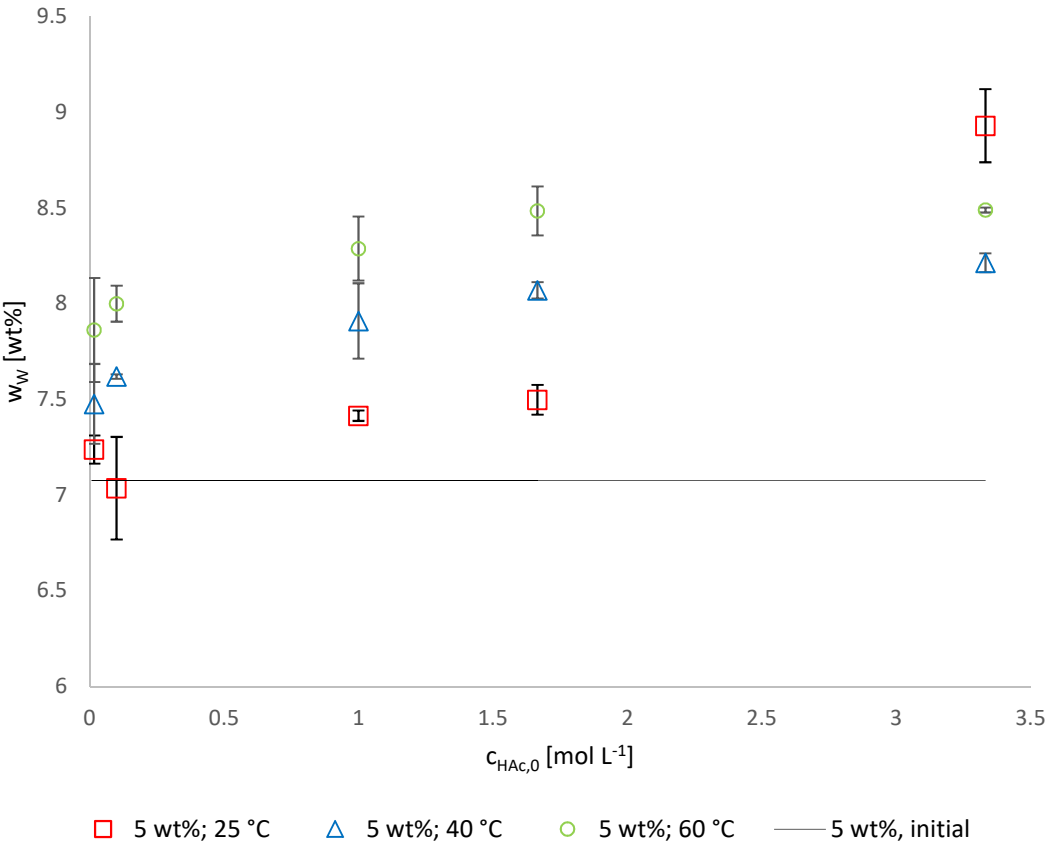

Figure 17: Mass fraction of water in the organic phase (w_W) in equilibrium after experiments on LLE at 25 °C, 40 °C, 60 °C with 5 wt% catalyst, related to initial aqueous acetic acid concentration

The solid line defines the mass fraction of water of the initial organic. This line is used as reference to analyze the effect of temperature and initial aqueous concentration of acetic acid on LLE of water. As can be seen an initial concentration of 3.330 mol L^{-1} leads to an increase of the water content in the organic phase from 7 in initial to 8.5 wt% in equilibrium. Generally, this increase of water content occurred over the whole range of analyzed initial concentrations of acetic acid. At the low initial concentrations of acetic acid (0.0167 and 0.100 mol L^{-1}), an increase already is found due to the better solubility of water in the organic phase at higher temperatures. A possible reason for the better solubility of water at higher initial concentrations of acetic acid is its polarity. Water can only be dissolved in polar solvents. In the initial state the organic phase consists only of catalyst and highly unpolar 1-octanol prior saturated with

water (reference line, section 3.2). The transferred acetic acid increases this total polarity of the organic phase and the solubility of water also increases. The points of water content at 40 and 60 °C show a comparable behavior. The curve of 25 °C does not fit this behavior, especially the second and the last point. This deviation is caused by errors during the experimental procedure. The high ranges of the errorbars at several points are caused by manual errors in measurement. During the experimental procedure, little amounts of samples were weight (about 200 mg). Errors in weighing could by the reason for the high deviations.

Figure 18 shows the mass fraction of water at w_{cat} equals to 20% related to the initial aqueous concentrations of acetic acid. Otherwise the same setting of temperatures was used as described in Table 4.

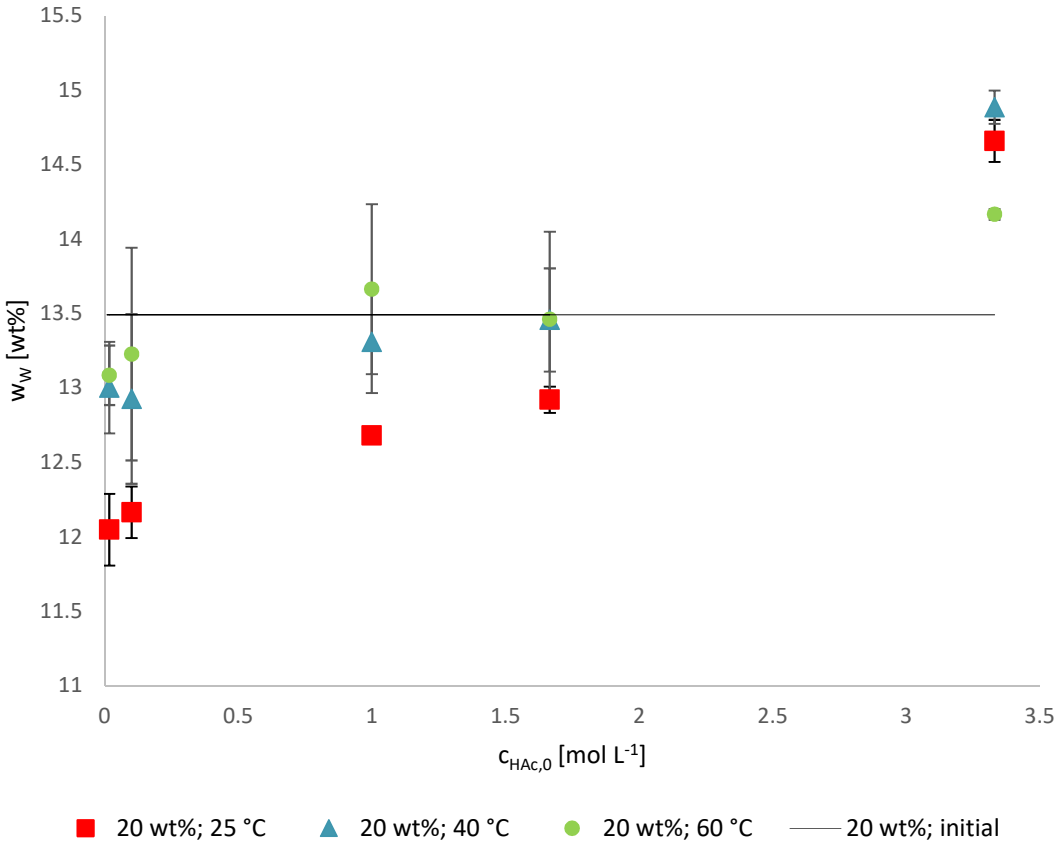

Figure 18: Mass fraction of water in the organic phase (w_W) in equilibrium after experiments on LLE at 25 °C, 40 °C, 60 °C with 20 wt% catalyst, related to initial aqueous acetic acid concentration

Low initial concentrations of acetic acid seem that transferred acetic acid decreases solubility of water, but high concentrations increase solubility of water. This is probably not the case in reality. Comparing the reference line of Figure 17 and Figure 18, shows, the main factor for the solubility of water is the mass fraction of catalyst. The problem with the mass fraction of catalyst is that little deviations in concentration lead to high variances in solubility of water. The real

concentration of catalyst of the samples, used in the LLE experiments could be higher than the one, used for the reference line. This would lead to a higher solubility of water. This problem could be avoided by preparation of single solutions of dissolved $NiDBSA_2$ in 1-octanol. Due to available equipment and drying time of three days, this was not always possible and time efficient. Although, a general trend of higher content of water in equilibrium at higher initial concentrations of acetic acid can be shown. An explanation for this phenomenon could be the polarity of acetic acid as described previously in Figure 17.

Due to physical extraction and reaction progress a change of densities could be measured (Figure 19).

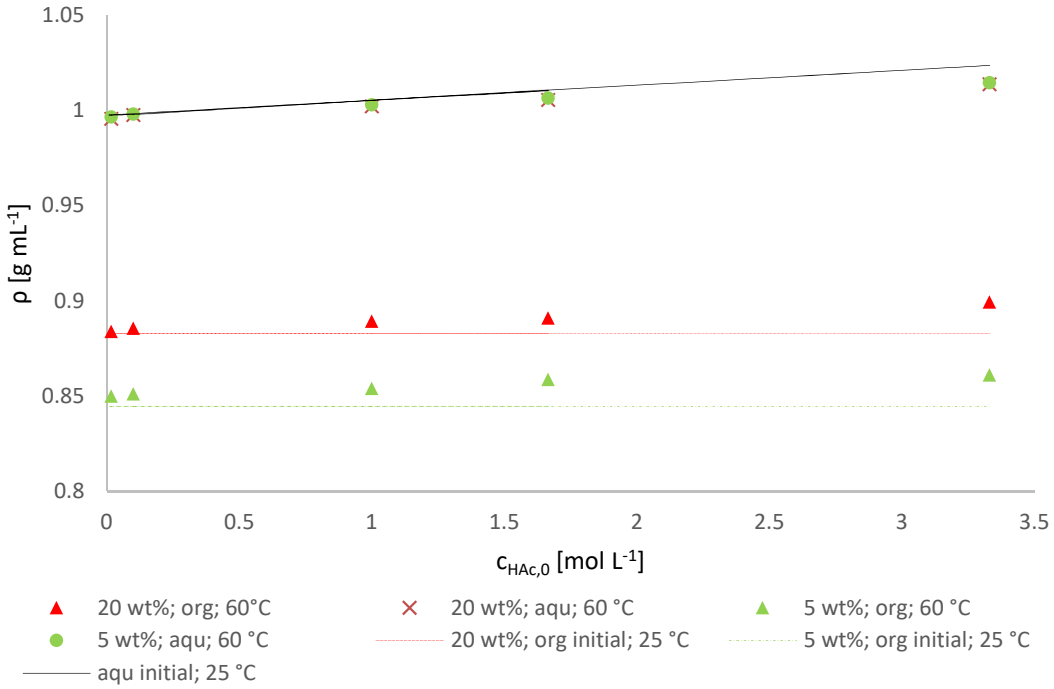

Figure 19: Comparison of densities of the phases in equilibrium after LLE experiments at 60 °C with their dedicated initial density, related to initial aqueous acetic acid concentration; temperature of density measurement: 25 °C

Figure 19 shows the behavior of the density of phases in equilibrium in respective to aqueous initial concentration of acetic acid at 60 °C. Density of the phases at equilibrium is measured at 25 °C after doing the experiments at 60 °C. This means, influence of temperature on density is not considered in these measurements, only the influence of different compositions. The solid and dashed lines define density of initial phases. The total density of the aqueous phase in equilibrium decreases with higher aqueous initial concentrations of acetic acid. This is because more acetic acid is transferred into organic phase. Acetic acid has a higher density than water, transferring acetic acid from the aqueous phase into the organic phase, leads to a decrease of total density. On the other side, the total density of the organic phase increases due to the

transferred acetic acid. The points of densities of the aqueous phases in equilibrium match each other, no matter which mass fraction of catalyst is used. This is because the aqueous initial concentration of acetic acid is low. Therefore, only little amount of acetic acid can be transferred. These experiments were also done at 40 °C and 25 °C. These measured points are all within the range of the deviation of points of the experiments at 60 °C to their reference line. Thus, less acetic acid is transferred at lower temperature. The results of experiments at 40 °C and 25 °C are not shown in separate diagram, because of their similar behavior compared to the results at 60 °C.

4.1.3 Influence of octyl acetate on distribution coefficients

To get an impression of the effect of octyl acetate on LLE of acetic acid, a separate series of experiments was done. In this series octyl acetate was added to initial solvent phase, resulting in a molar ratio 1-octanol to octyl acetate of 10:1. The experiments were done at 25 °C. Like in the analysis of the experiments without initial octyl acetate, the concentration of acetic acid in the organic phase was computed by addition of the measured concentrations of octyl acetate and acetic acid, but also the subtraction of the concentration of the added octyl acetate (Equation 13).

$$c_{HAc_{org,tr+OctAc}} = c_{HAc,org} + c_{OctAc} - c_{OctAc,add} \quad (13)$$

The distribution coefficients are determined like in Figure 15 and compared to the ones without initial octyl acetate (Figure 20).

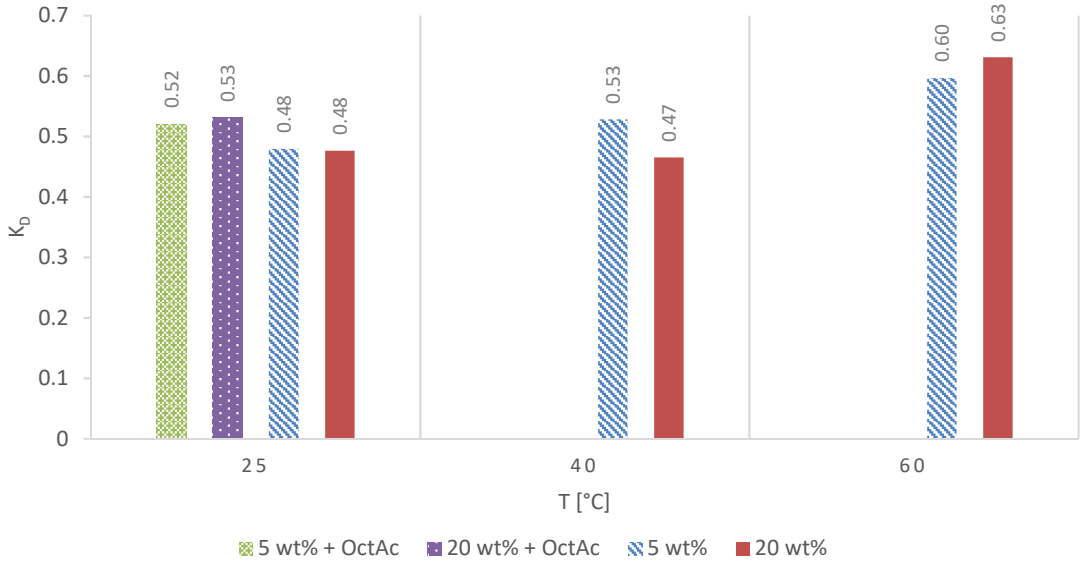

Figure 20: Comparison of distribution coefficient K_D at all analyzed combinations of temperature and mass fraction of catalyst with compared distribution coefficient at 25 °C with initial octyl acetate (molar ratio of OctAc (added) : Oct = 1 : 10)

The first two bars of 25 °C define the distribution coefficients with initial octyl acetate. Comparing with the distribution coefficients without initial octyl acetate, a slight increase can be obtained for both mass fractions of catalyst, thus octyl acetate increases solubility of acetic acid in solvent phase. Which is a benefit for recovery efficiency of the reactive extraction. Due to the low effect, increase of distribution coefficient by octyl acetate is neglected in kinetic modeling (section 5.1).

4.2 Analysis of experimental data of kinetics

The progress of the esterification is evaluated over five hours. Concentrations of acetic acid in both phases and octyl acetate in the organic phase are merged in one diagram for each temperature and used mass fraction of catalyst, because of their similar range of concentration. Depending on temperature and concentration of catalyst, the progress of the reaction behaves differently. To show the range of different kinetic behavior, diagrams of 5 wt% catalyst at 25 °C (Figure 21) and 20 wt% at 60 °C (Figure 22) are shown.

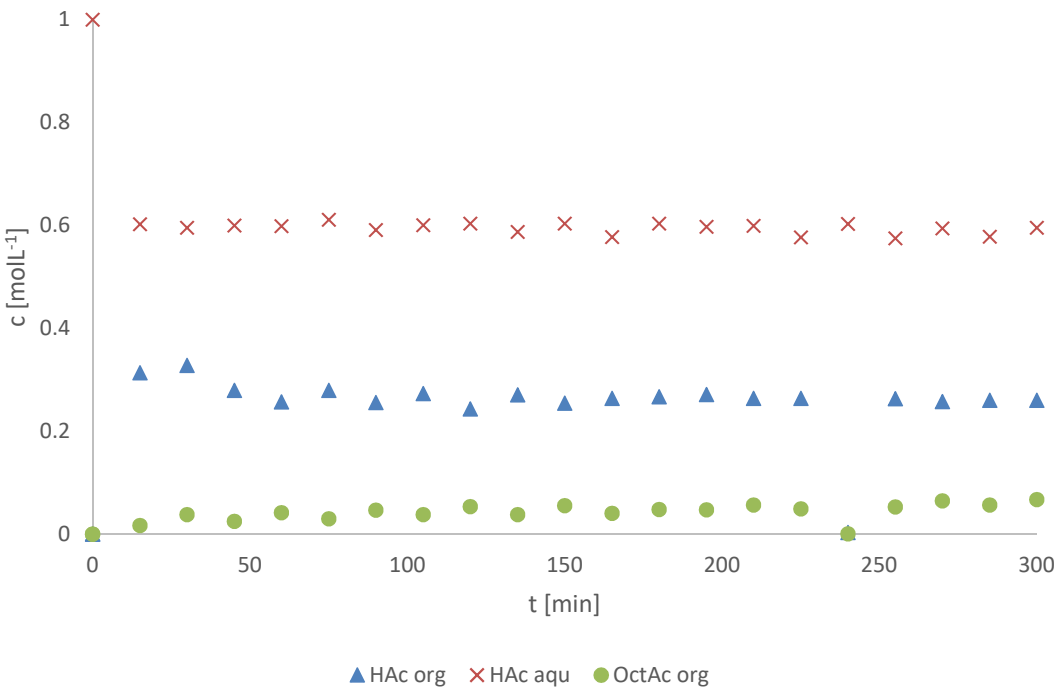

Figure 21: Concentrations profiles of acetic acid in aqueous and organic phase and octyl acetate in organic phase at 25 °C and 5 wt% catalyst during 300min

Figure 21 shows that a minor amount of octyl acetate is formed by the combination of 25 °C and 5 wt% catalyst. At time zero, the concentration of acetic acid in the aqueous phase is computed by Equation 11 (section 3.3.2). The concentration of acetic acid in the organic phase is initially zero. The same is valid for the concentration of octyl acetate. As seen at the points

of 15 and 30 minutes, equilibrium of physical extraction is reached and 30 minutes of shaking in the experiments on LLE (section 3.3.2) are reasonable. At minute 240, a gap in the concentration of acetic acid acetate in the organic phase and a value of zero for the concentration of octyl acetate appears. This is caused by errors in measurement of the GC device.

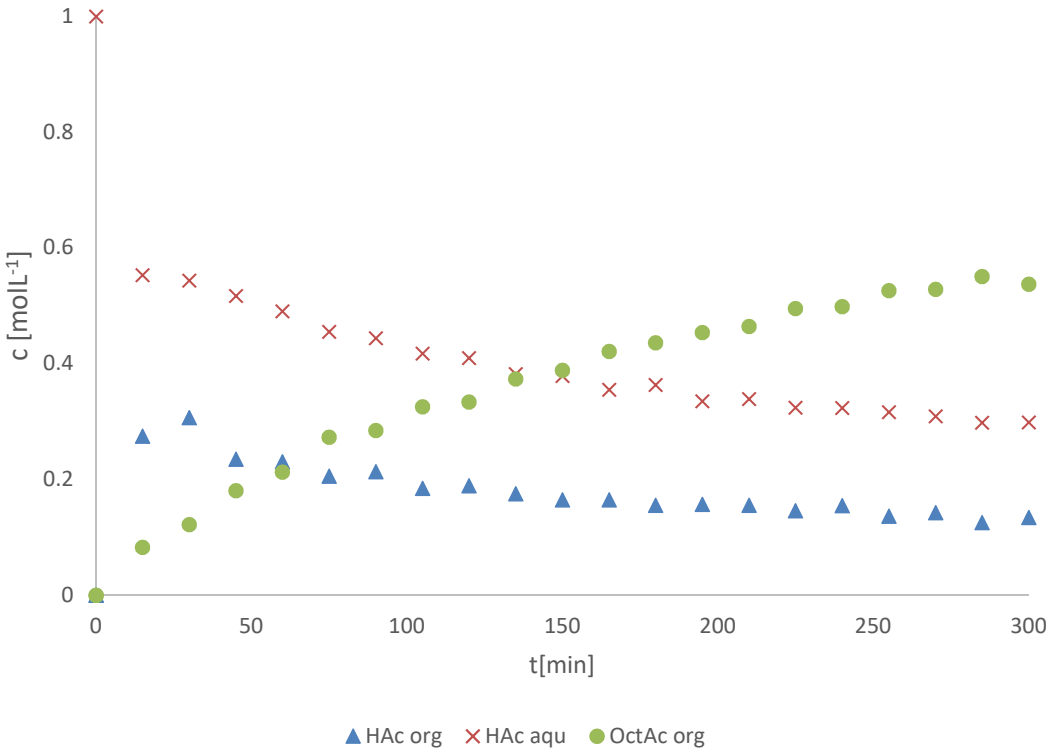

Figure 22: Concentrations profiles of acetic acid in aqueous and organic phase and octal acetate in organic phase at 60 °C and 20 wt% catalyst during 300 min

The kinetic behavior at 60 °C and 20 wt% catalyst is shown in Figure 22. Compared to Figure 21, more octyl acetate is formed in 300 minutes. More than half of acetic acid is consumed to octyl acetate. As seen at the points of 30 minutes, less than 10 % of acetic acid has reacted to octyl acetate. This reactive part is neglected in the determination of the distribution coefficient.

To compare all analyzed combinations of temperature and mass fraction of catalyst, parameters like conversion and recovery are computed for each combination. The analyzed chemical system is assumed as quasi-monophasic. The molar amount in the quasi-monophasic system can be defined as the sum of the molar amount of the organic and aqueous phases, as described in Equation 14.

$$n_{HAc,mono} = n_{HAc,org} + n_{HAc,aqu} \quad (14)$$

These molar amounts can be expressed be the measured concentrations and their dedicated volumes. The volume of the quasi-monophasic system is defined as the sum of the volume of organic and aqueous phase (Equation 15).

$$c_{HAc,mono}(V_{org} + V_{aqu}) = c_{HAc,org} V_{org} + c_{HAc,aqu} V_{aqu} \quad (15)$$

Volume is assumed to stay constant during the experiment and ratio of organic versus aqueous of 1:1 is used. Thus, volumes can be eliminated and the concentration of acetic acid in the quasi-monophasic system can be calculated (Equation 16).

$$c_{HAc,mono} = \frac{c_{HAc,org} + c_{HAc,aqu}}{2} \quad (16)$$

Conversion is defined by the monophasic concentration of acetic acid (Equation 17).

$$X_{HAc} = \frac{c_{HAc,mono,0} - c_{HAc,mono}}{c_{HAc,mono,0}} \quad (17)$$

Where $c_{HAc,mono,0}$ is defined as the initial quasi-monophasic concentration of acetic acid.

Conversion only considers reacted acetic acid, but not acetic acid, transferred into the solvent phase. This is considered by recovery R, which is defined by the sum of the concentration of octyl acetate and transferred acetic acid in the numerator (Equation 18).

$$R = \frac{c_{OctAc} + c_{HAc,org}}{c_{HAc,aqu,0}} \quad (18)$$

Conversion and recovery are calculated for all combinations of temperature and mass fraction of catalyst.

To analyze impacts of catalyst and temperature on the kinetic behavior of the system conversion and recovery after 300 minutes, the end of the kinetic experiment, are shown (Figure 23).

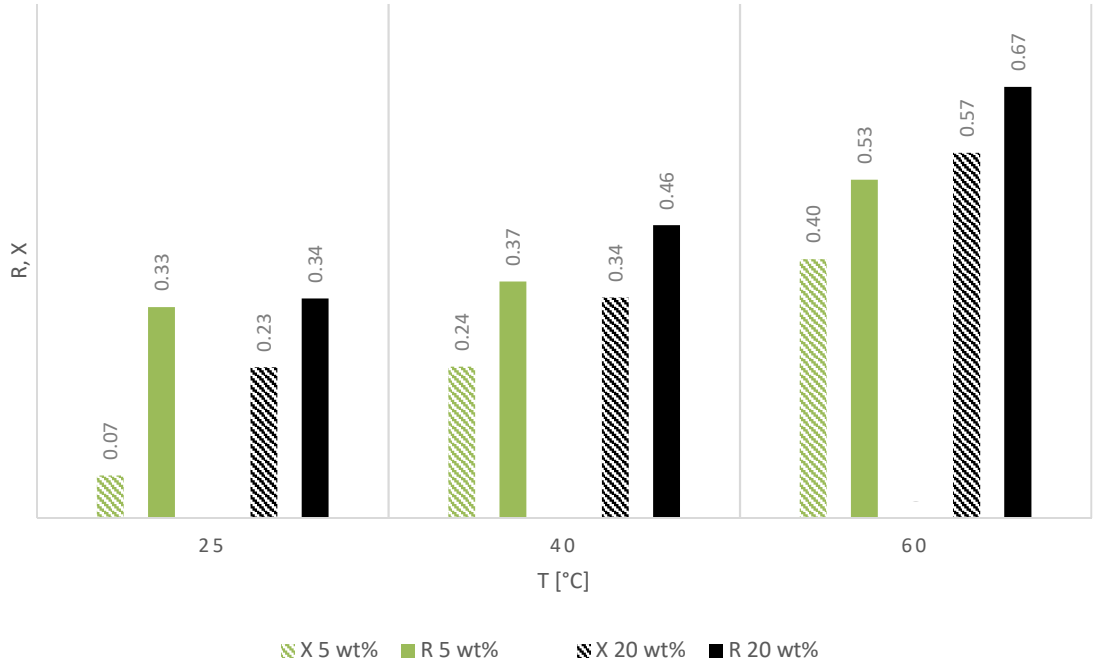

Figure 23: Comparison of conversion and recovery after 300 minutes (end of kinetic experiment) of all analyzed combinations of temperature and mass fractions of catalyst.

Conversion and recovery increase with temperature. This is expected, because elevated temperature enhances reaction rate and physical extraction (Figure 20). Little conversion is achieved at 25 °C and 5 wt% catalyst, thus almost no reaction appears. If conversions are subtracted from their corresponding recovery, the contribution of physical extraction to recovery can be estimated. A constant value of approximately 0.12 can be calculated (except for 25 °C and 5 wt% catalyst), which means 12 % of total acetic acid is recovered by physical extraction only. This constant value approves octyl acetate at the appearing concentration has no crucial influence on physical extraction at any temperature. Dividing this value by recovery, the relatively contribution of physical extraction can be estimated. For the highest value of recovery (60 °C, 20 wt%) about 15 % is caused by physical extraction. The residual and bigger part is caused by reaction. At 25 °C and 20 wt% catalyst, physical extraction contributes approximately 30 % to recovery. The contribution of physical extraction generally decreases by conversion. Comparing conversion of 20 wt% catalyst and 40 °C (0.34) with the one of 5 wt% catalyst and 60 °C (0.40), a higher conversion is recognized despite less catalyst. This can also be seen by comparing other temperatures and mass fractions of catalyst.Thus, demand of catalyst can be reduced by increasing temperature.

Composition of extract (loaded solvent) would be important for recycling of solvent by reactive distillation (chapter 1) and is shown as mass fraction in Figure 24.

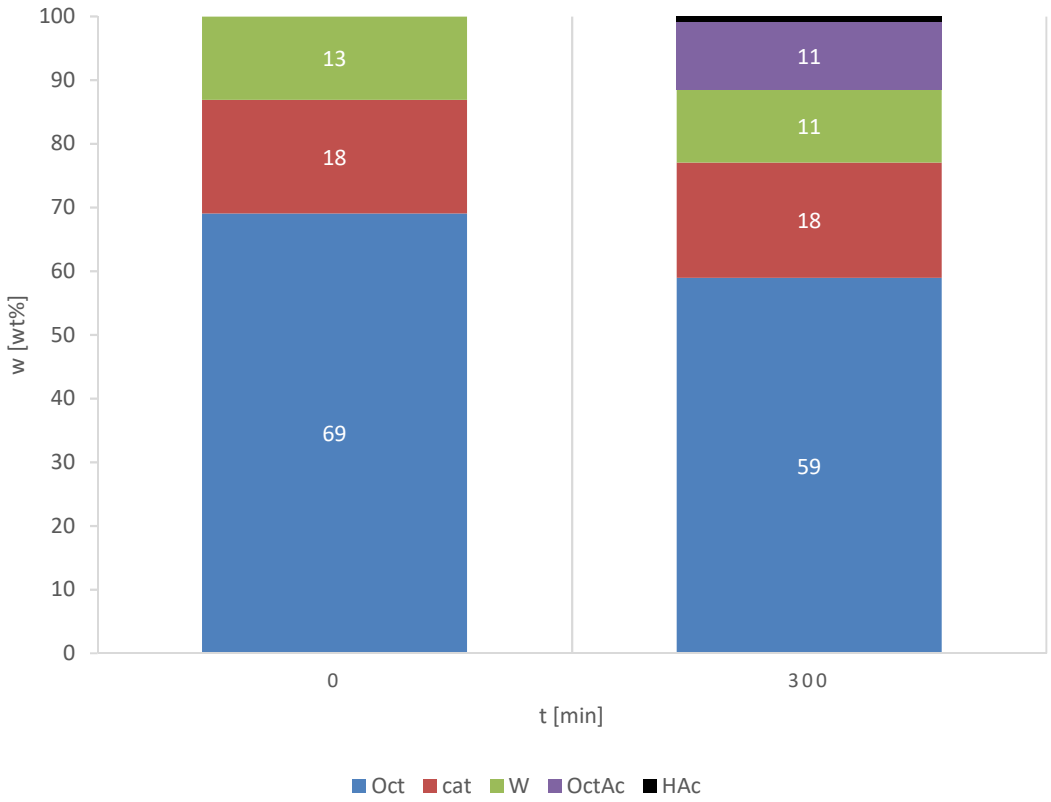

Figure 24: Initial composition and composition after 300 minutes (end of kinetic experiment) of solvent phase; 60 °C; 20 wt% catalyst;

Initial composition and composition after 300 minutes of solvent phase at 60 °C and 20 wt% of catalyst are shown in Figure 24. The initial solvent phase consists of 1-octanol with dissolved water and catalyst. The mass fraction of water decreases from 20 to 18 wt% due to prior saturation of water of the solvent phase (section 3.2). The esterification of acetic acid to octyl acetate consumes a corresponding part of 1-octanol. Octyl acetate also decreases solubility of water, which contradicts the water coextraction effect seen in experiments on LLE in section 3.3. The thin black stripe on top of the column of 300 minutes shows the mass fraction of dissolved acetic acid, which is about 1 wt%. The low amount of dissolved acetic acid confirms the conclusion that recovery of acetic acid is mainly driven by chemical reaction.

For kinetic modeling of this type of chemical system, the equilibrium state must be known. This state can be determined by data generated by experiments in shaking water bath. Measured concentrations after 24 and 48 h were constant, thus equilibrium state was reached for 40 and 60 °C. At 25 °C, constant concentration is measured because of minor reaction rate (also seen in Figure 21) not because of reaching equilibrium. Conversion and recovery are computed for all analyzed compositions of temperature and mass fractions of catalyst (Equation 17 and 18). The results are shown in Figure 25.

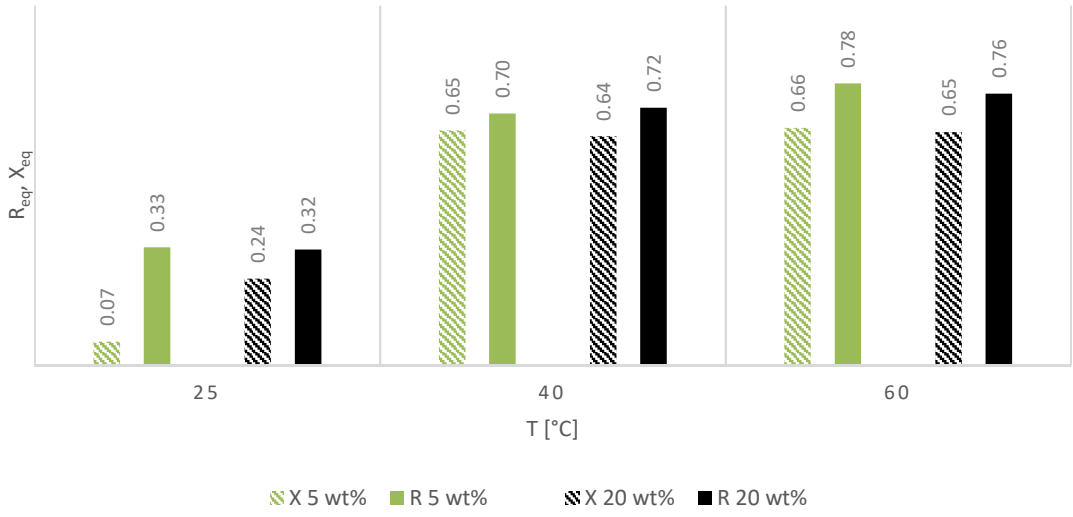

Figure 25: Comparison of conversion and recovery in equilibrium of all analyzed combinations of temperature and mass fractions of catalyst.

Little difference in conversion and recovery is shown at 40 °C and 60 °C for equilibrium states. At 25 °C, similar values are seen compared to the ones after 300 minutes, the end of the kinetic experiment (Figure 25). Seemingly, equilibrium could not be reached at 25 °C. Mass fraction of catalyst does not impact equilibrium conversion at 40 and 60 °C. This is expected, because catalyst does not influence equilibrium of a reaction. Values of conversions are only slightly lower than the ones of recoveries, thus very little acetic acid is dissolved in extract.

Concentration of 1-octanol and content of water in the organic phase show high deviations in double or triple determination. A decrease of both could be identified. Because of these high deviations (standard deviation of water up to 12 %) and discontinuous decrease, both cannot be used for modeling.

Formation of octyl acetate and consumption of acetic acid and 1-octanol lead to changes of volume. This change of volume is determined by weight and density of the separated phases after the final sample at 300 minutes. The final volume of each phase could be computed by using Equation 19 and 20.

$$V_{org,fin} = \frac{m_{total,fin}\left(\frac{m_{org,fin}}{m_{org,fin}+m_{aqu,fin}}\right) + \sum m_{Sample,org}}{\rho_{org,fin}} \quad (19)$$

$$V_{aqu,fin} = \frac{m_{total,fin}\left(\frac{m_{aqu,fin}}{m_{org,fin}+m_{aqu,fin}}\right) + \sum m_{Sample,aqu}}{\rho_{aqu,fin}} \quad (20)$$

Initial volumes are calculated as the averages of the initial volumes of each of the two experiments, due to the double determination. The final volumes are single values because only one experiment lasted on for 300 minutes. During the kinetic experiments, about l0 ml of each phase was taken for sampling. An estimation of this volume of the samples was done by weighing them and assuming constant densities of the samples during the experiment. Densities could not be measured because of the low amount of sample. Comparing densities of the initial phases and final phases, changes of maximum 0.5 % could be measured. Thus, changes in densities can be neglected. For this calculation densities at 25 °C of separated phases after the final samples were used. This calculation was done for all kinetic experiments. Changes of volumes of up to 3 mL were estimated. In the experiment with 5 wt% catalyst and 60 °C, 7 ml was obtained at the organic phase. This outlier is caused by an error is separation. Separation of the phases was challenging, as in some cases foam was formed between the two phases. This foam was centrifuged. During this procedure, the foam was filled in test tubes for centrifuging and separated with a syringe afterwards. In this procedure an additional error was inevitable. Although potential high errors in measuring, little change in volume can be assumed and thus are neglected in kinetic modeling (chapter 5). The possibility of gravitational separation of the phases by centrifuge proves, no microemulsion is formed at any combination of temperature and mass fraction of catalyst.

Knowing the finale volume and the concentrations at the end of the 300 minutes, an error in mass balance $E_{m,HAc,300}$ of acetic acid can be calculated by Equation 21. Acetic acid dissolved in both phases and bound in octyl acetate was considered. The initial amount of acetic acid is weight in the syringe.

$$E_{HAc,300} = \frac{n_{HAc,0} - c_{HAc,aqu,300} V_{aqu,fin} - c_{HAc,org,300} V_{org,fin} - c_{OctAc,org,300} V_{org,fin}}{n_{HAc,0}} \quad (21)$$

The result of this error calculation is 4.03 to maximum of 12.62 %. This maximum error appeared at the experiment at 40 °C and 5 wt% of catalyst.

To check if any acetic acid, water or 1-octanol evaporated through the cooling system, a total mass balance was calculated (Equation 22).

$$E_{total} = \frac{m_{HAc,0} + m_{org,0} + m_{aqu,0} - m_{total,fin}}{m_{total,fin}} \quad (22)$$

$E_{m,total}$ defines the error of the total mass balance. $m_{org,0}$ defines the mass of the initial organic phase, $m_{aqu,0}$ defines the initial aqueous phase, which was pure water in the kinetic experiments, and $m_{HAc,0}$ is the mass of acetic acid, injected in the system by syringe. The mass of both phases after the last sample before phase separating is defined as m_{final}. Total mass errors of all experiments were below 0.5 %. Thus, no substance was lost during the experiment.

4.3 Determination of CMC

As described in section 2.4, the critical micelle concentration (CMC) is an important factor to understand the behavior of a micellar system. CMC can be computed by measuring the surface tension of various concentrations of the surfactant. Dissolving of $NiDBSA_2$ in water was not possible in significant or measurable concentrations and a CMC of catalyst in water could not be determined. As described in section 2.4, $NiDBSA_2$ tends to form reverse micelles in a hydrophobic (organic) continuous phase. To check this possible phenomenon, the surface tensions of various concentrations of dissolved catalyst in 1-octanol and rinsed with water were measured. The measurements were done at a constant temperature of 25 °C. For drawing the diagram, w_{cat} had to be transferred to c_{cat}. Since surface tension is plotted in respect to c_{cat} in logarithmic scale, the concentration of w_{cat}= 0 is defined as 1.00 10^{-5} mol L^{-1}. (Equation 23, Table 10, Figure 26)

$$c_{cat} = 1000\ \rho_{org} \left[\frac{g}{mL}\right] w_{cat}\ M_{cat} \tag{23}$$

Table 10: Concentration of $NiDBSA_2$ c_{cat} calculated from mass fraction w_{cat} for surface tension

w_{cat} [%]	c_{cat} [mol L^{-1}]
0	1.00 10^{-5}
5	5.77 10^{-2}
10	1.19 10^{-1}
28	3.51 10^{-1}

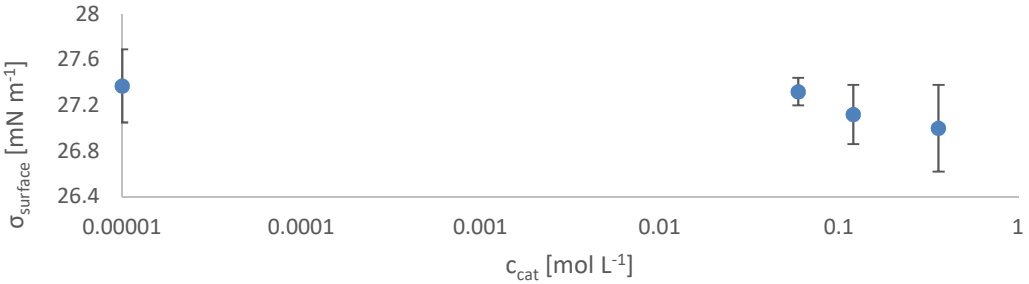

Figure 26: Surface tension with respect concentration of catalyst in 1-octanol saturated with water in logarithmic scale at 25 °C

Figure 26 shows the surface tension related to concentration of catalyst in 1-octanol in logarithmic scale. The point at the lowest concentration is the point of pure 1-octanol. The other values of concentration are the points of 5, 10 and 28 wt% mass fractions of catalyst in 1-octanol. The catalyst reduces the surface tension slightly, but the decrease is within the standard deviation of the surface tension of 28 % mass fraction, which was the concentration of catalyst in 1-octanol at maximum solubility. Therefore, analyzing an even higher concentration of catalyst was not possible and a CMC of the catalyst for reverse micelles in 1-octanol cannot be determined.

4.4 Analysis of experimental data of interfacial tension

The catalyst could not be dissolved in water. This meant, CMC could not be determined. Another possibility to generate knowledge of the behavior of catalyst in the system is the interfacial tension. Interfacial tension is measured at the interface of organic and aqueous phase. Before measuring, the procedure of the LLE-experiments (section 3.2) was done at 25 °C. This ensured the organic phase was at equilibrium with the aqueous phase. Because of the residual DBSA in the aqueous phase after separation (Figure 10), a measurement of interfacial tension of both phases in equilibrium was not possible and pure water was used as aqueous phase for measurement. To check the dependency on temperature of the dynamic interfacial tension, the whole procedure was done for three points at 60 °C. w_{cat} is converted in c_{cat} by Equation 23 (Table 11).

Table 11: c_{cat} calculated from w_{cat} for dynamic interfacial tension

w_{cat} [wt%]	c_{cat} [mol L^{-1}]
0	$1.00\ 10^{-5}$
$5\ 10^{-3}$	$5.86\ 10^{-5}$
$5\ 10^{-2}$	$5.86\ 10^{-4}$
2.5	$2.95\ 10^{-2}$
5	$5.77\ 10^{-2}$
10	$1.19\ 10^{-1}$
20	$2.49\ 10^{-1}$
28	$3.51\ 10^{-1}$

Figure 27 shows the interfacial tension dependent on the concentration of catalyst in the organic phase. The point at the lowest concentration defines the interfacial tension without catalyst. The red crosses define the interfacial tension at 60 °C.

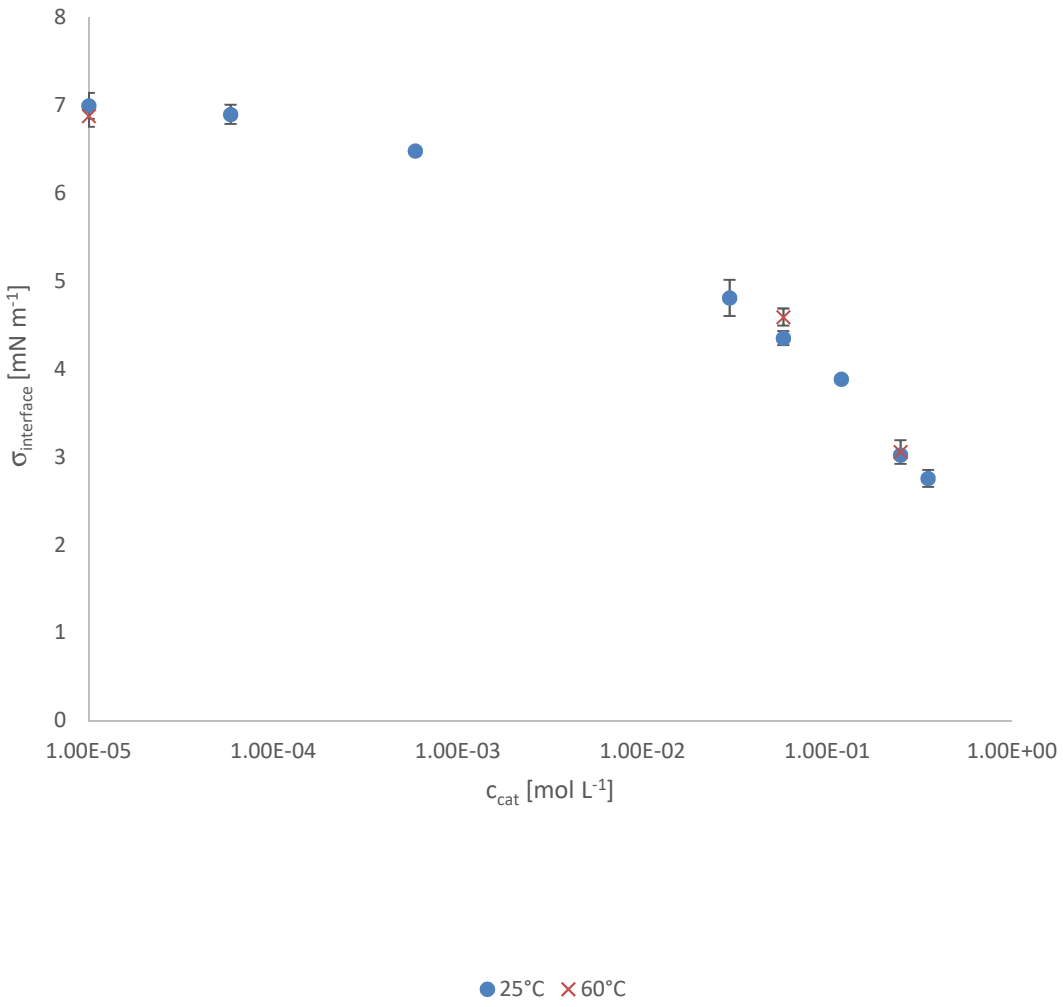

Figure 27: Interfacial tension against concentrations of catalyst in logarithmic scale at 25 °C and 60 °C; continuous phase: water; dispersed phase: organic phase after LLE experiment, containing 1-octanol, catalyst, transferred acetic acid and water

Obviously, there is hardly any dependency on temperature of the dynamic interfacial tension, as the points match with the ones of the same concentration of catalyst at 25 °C. The decrease of interfacial tension by concentration starts at a value of about 10^{-4} mol L^{-1} catalyst, which equals to a w_{cat} = 0.05 wt%. At the last point (28 wt%) the dynamic interfacial tension reaches the lowest value of less than 3 mN m^{-1}, which is a decrease of more than a half compared to the 7 mN m^{-1} of pure 1-octanol. Using 5 % catalyst, the dynamic interfacial tension decreases to a value of about 4.3 mN m^{-1}. A lower dynamic interfacial tension means, a less stiff interface, which enables a better transfer of substances between the phases. Additionally, a higher amount of catalyst generally enhances the reaction. Reduction of approximately 38 % of interfacial tension by using 5 wt% of catalyst confirms results found in previous investigations [1].

5 Kinetic Modeling and order of catalyst

A modeling approach for the reactive kinetics was developed based on the obtained experimental data. This includes the application of the first order kinetics introduced in chapter 2 and determination of the order of catalyst.

5.1 Reaction kinetic modeling

The metallosurfactant catalyst $NiDBSA_2$ reduces interfacial tension (Figure 27) while preventing emulsification. This results in a quasi-monophasic system. The chemical reaction kinetics of such a homogenous system allows application of the kinetic approach described in section 2.5. All three introduced rate laws (Equation 6, 7 and 8) were tested with the obtained experimental data. To optimize the kinetic model on the concentration profile of octyl acetate, the conversion is redefined based on the product concentration. (Equation 24).

$$X_A = \frac{c_R}{c_{A,0}} \tag{24}$$

This is possible, as no competing or parallel reaction appears in the system. If the computed value for k_1 remains constant, the chosen model is suitable for describing the system. The rate law assuming second order regarding the acetic acid concentration (Equation 8) shows best performance. According to this, forward reaction is a second order reaction of acetic acid and the backward reaction behaves like a first order reaction of octyl acetate. The reaction rate constant for forward reaction, k_1 can be computed as a function of time and conversion, computed by measured concentrations with Equation 25 in Table 2.

$$k_1 = \frac{1}{D_1 t} \ln \frac{(2f_a X_A + f_b - D_1)(f_b + D_1)}{(2f_a X_A + f_b + D_1)(f_b - D_1)} \tag{25}$$

$$D_1 = \sqrt{{f_b}^2 - 4 f_a f_c}$$

k_1 behaves constant over time. Outliers at earlier timesteps are caused by mixing effects at the start of the experiment. For determining the modeled conversion of acetic acid, the average of all computed values of k_1 in the constant region without outliers is used. Conversion of acetic acid can be modeled by rearrange Equation 25 (k_1). Since no side reaction appears in this

system, the concentration of octyl acetate is the difference between initial and current concentration of acetic acid (Equation 26).

$$c_{OctAc,mono} = c_{HAc,mono,0} - c_{HAc,mono} \quad (26)$$

This difference in concentration of acetic acid can also be expressed by conversion described in Equation 17 and inserted in Equation 26 to arrive at Equation 27.

$$c_{OctAc,mono} = X_{HAc}\, c_{HAc,mono,0} \quad (27)$$

Octyl acetate is only soluble in the organic phase. Thus, the total molar amount of octyl acetate in the quasi-monophasic system is present only in the organic phase after phase separation (Equation 28).

$$c_{OctAc,mono}\left(V_{org} + V_{aqu}\right) = c_{OctAc,org}\, V_{org} \quad (28)$$

Constant volume during the reaction and volume ratio of organic to aqueous of 1 is assumed. Due to this assumption, volumes can be eliminated in Equation 28 and the resulting equation can be inserted in Equation 27, which leads to Equation 29.

$$c_{OctAc,org} = 2\, X_{HAc}\, c_{HAc,mono,0} \quad (29)$$

Equation 29 is used to compute the concentration of octyl acetate from modeled conversion.

For computation of the concentration of acetic acid in organic and aqueous phase, distribution coefficient of acetic acid $K_{D,HAc}$ is needed (Equation 30).

$$K_{D,HAc} = \frac{c_{HAc,org}}{c_{HAc,aqu}} \quad (30)$$

Combined with molar balance described by Equation 14 and 15 and $K_{D,HAc}$, the concentrations of acetic acid in organic and aqueous phase can be computed (Equation 31 and 32).

$$c_{HAc,org} = \frac{2\, c_{HAc,mono}\, K_{D,HAc}}{K_{D,HAc} + 1} \tag{31}$$

$$c_{HAc,aqu} = 2\, c_{HAc,mono} - c_{HAc,org} \tag{32}$$

Computed concentrations can be compared with concentrations experimentally determined. This is shown exemplarily with the data of the kinetic experiment at 60 °C and 20 wt% catalyst (Figure 28)

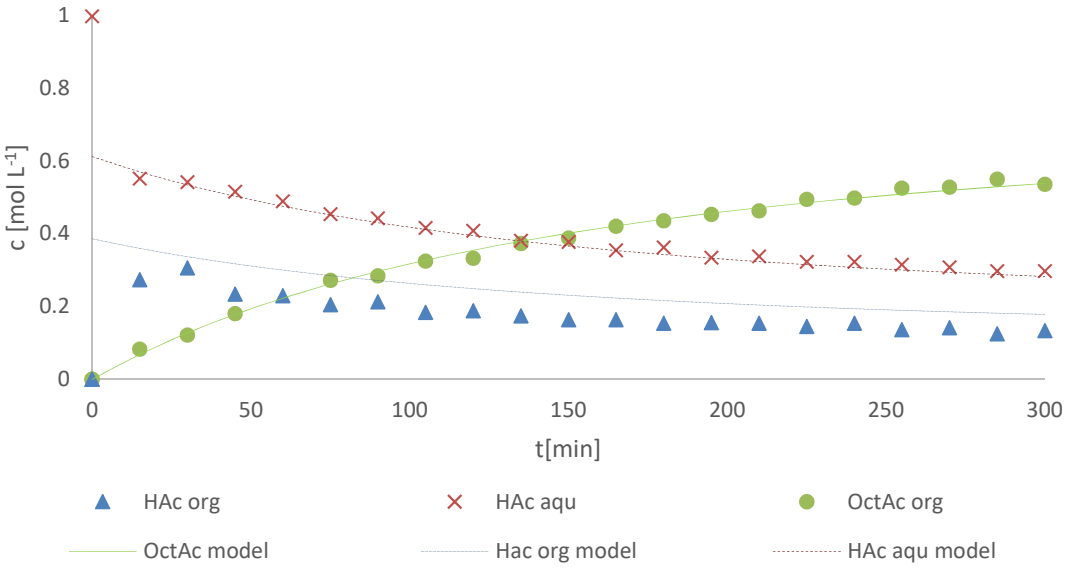

Figure 28: Concentration profiles of acetic acid in aqueous and organic phase and octyl acetate in organic phases, compared with their modeled concentrations at 60 °C and 20 wt% catalyst

The discrete points in the diagram of Figure 28 show the experimental concentrations of the experiments. Solid and dashed lines define the modeled concentrations. The model fits the measured data accurately. The reaction within the first 15 min of the reaction cannot be described with the chosen model. This is a result of the predominate physical extraction in the system. Computing the concentrations of acetic acid in both phases initially equilibrium of physical extraction was assumed. The model fits the concentrations of octyl acetate and acetic acid in aqueous phase and shows parallelism to the concentration of acetic acid in the organic phase. This parallelism is caused by mass balance error of acetic acid in the experimental data. The highest values of mass balance errors of acetic acid were determined at 40 °C (12.62 %). Figure 29 shows experimental and modeled concentrations at 40 °C and 20 wt% catalyst. The model appeared to be most inaccurate at this case.

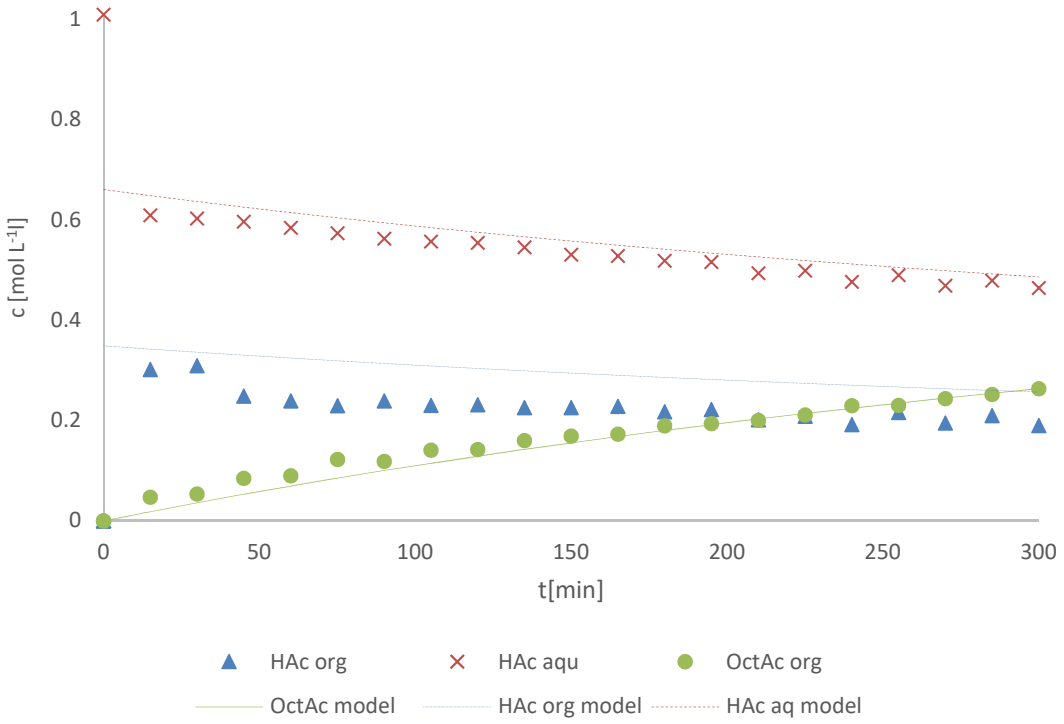

Figure 29: Concentration profiles of acetic acid in aqueous and organic phase and octyl acetate in organic phases, compared with their modeled concentrations at 40 °C and 20 wt% catalyst

Inaccuracies appear especially in the first half of the analyzed time interval at the concentration of octyl acetate. According to experimental data, the reaction is faster than modeled at the beginning. After 250 minutes, experimental and modeled data match each other. Longer time intervals must be analyzed to gain certainty, whether the phenomenon after 250 minutes is an intersection or convergence of experimental and modeled data. A possible reason for this error in the model could be deviations of the equilibrium conversion. The experimental determination of the equilibrium conversion via acetic acid with small reaction volumes is prone to errors. Future approaches should consider the determination based on the reaction product (octyl acetate).

Accurate modeling of the concentration of octyl acetate was possible at all temperatures and mass fractions of catalyst. Deviations of the modeled concentrations of acetic acid to the experimental ones appeared at all analyzed cases. All other combinations of temperature and mass fraction of catalyst are shown in Appendix C. Reaction rate constants k_1 (forward; [L mol^{-1} min^{-1}]), k_2 (backward; [min^{-1}]) and equilibrium constants K_{eq} [L mol^{-1}] of the analyzed cases are summarized in Figure 30, Figure 31 and Figure 32.

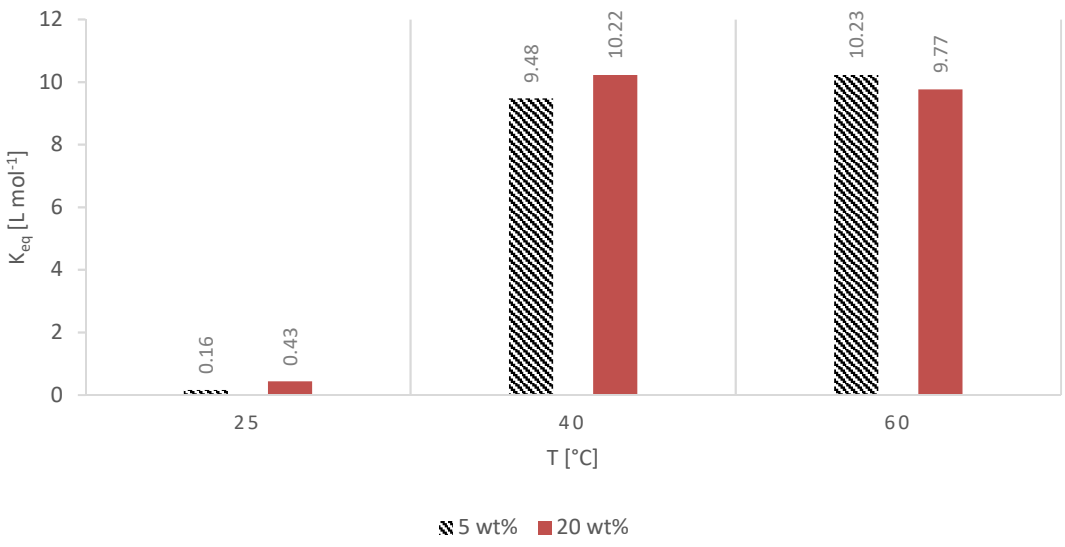

Figure 30: Equilibrium constant K_{eq} [L mol^{-1}] of the esterification of acetic acid with 1-octanol in respective to temperature

Figure 30 confirms, equilibrium is not reached at 25 °C after 24 hours. Equilibrium constants are similar at 40 and 60 °C. Generally, K_{eq} behaves similar to X_{Ae} and R_{Ae}. This is expected, because X_{Ae} and K_{eq} are directly related to each other (Table 1).

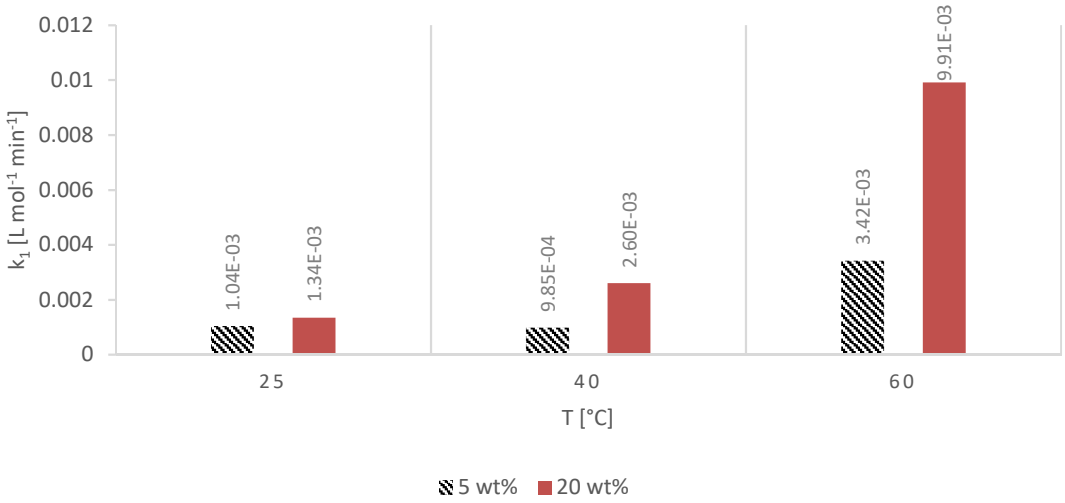

Figure 31: Reaction rate constant k_1 (forward; [L mol^{-1} min^{-1}]) of the esterification of acetic acid with 1-octanol in respective to temperature

Figure 31 shows the reaction rate constant dependent on temperature. Forward rate constants increase exponentially with temperature at 20 wt% catalyst, which could be modeled by the Arrhenius Equation. However, rate constants of 5 wt% catalyst do not match a continuous growth, because the lowest rate constant was found at 40 °C.

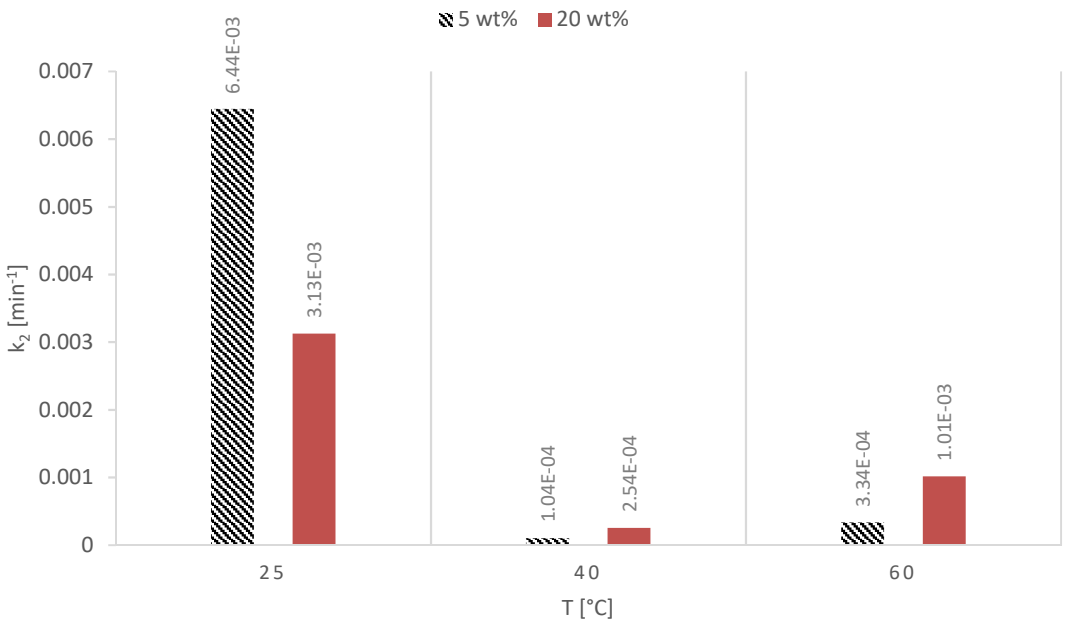

Figure 32: Reaction rate constant k_2 (backward; [min^{-1}]) of the esterification of acetic acid with 1-octanol in respective to temperature

The computed values of the backward reaction rate, related to temperature, is shown by Figure 32. The high reaction rates for backward reaction at 25 °C are caused by failure of reaching equilibrium. Reaction rates of backward reaction also increase by temperature as seen for forward reaction rate. Invalid data, especially at 25 °C, makes it impossible to identify any trend for modeling.

Values of equilibrium constants and backward reaction rate constants at 25 °C show, equilibrium was not reached in experiments and determination of equilibrium at 25 °C would take more time than three days. However, Figure 29 shows that reactive extraction is highly inefficient at 25 °C. Thus, further investigations at temperatures like 25 °C are not necessary.

5.2 Determination of the order of catalyst

According to section 2.6, the effect of catalyst on the kinetics of a chemical reaction can be estimated by applying a graphical method. The order of catalyst was determined by manual fitting of the parameter γ of the normalized time tc_{cat}^{γ}. This is shown exemplary at the data of 60 °C (Figure 33).

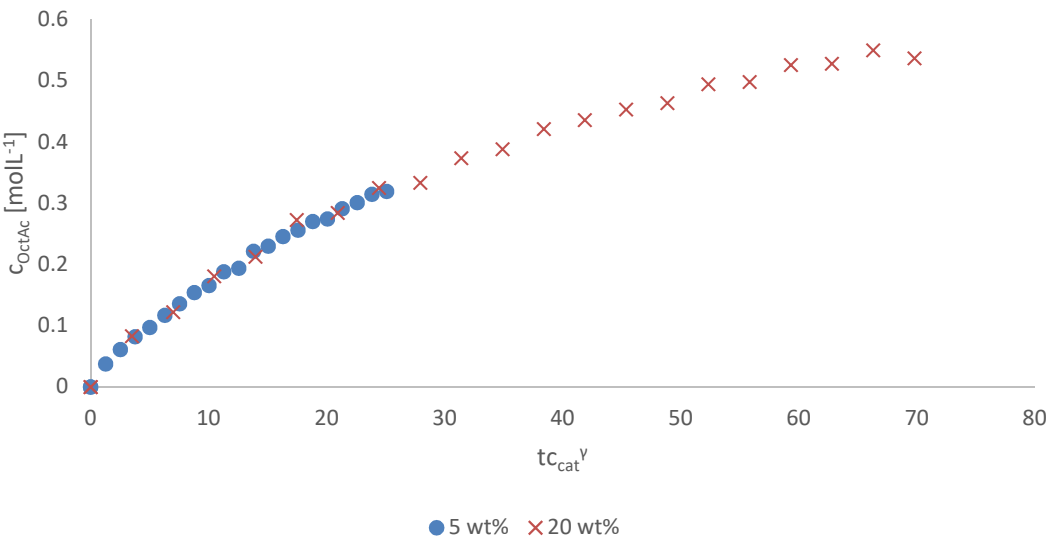

Figure 33: Determination of order of catalyst γ; time-normalized abscissa at 60 °C

As seen in Figure 33, both curves can be fitted in each other by using the normalized time with the order of catalyst γ. This method can also be applied at the data of experiments at 25 and 40 °C (Table 12).

Table 12: determined order of catalyst γ at analyzed temperatures (25, 40, 60 °C)

Order of catalyst γ	Temperature [°C]
0.6	25
0.86	40
0.7	60

The fitting at 25 °C was not accurate, this is because the concentration of octyl acetate is very low at 5 wt% of catalyst. γ should not depend on temperature. This could be the case, values for γ deviate from each other, but a trend with temperature cannot be found.

6 Discussion

In previous research, a reactive system with DBSA as catalyst and a solvent phase composed by 1-octanol and *n*-undecane was analyzed [6]. Due to low solubility of acetic acid in solvent phases containing *n*-undecane, minor superposing physical extraction of acetic acid occur and recovery approximately equals conversion (Figure 12, [6]). In that previous investigation a dependency of conversion on concentration of 1-octanol was found. In the present investigation, the opposite was found. Due to the high molar excess of 1-octanol, changes in 1-octanol concentration seemingly has little effect on the reaction kinetics and the equilibrium. 1-octanol does not affect kinetics or equilibrium. This contradiction could be caused by composition of the solvent phase. In the present investigation, undiluted 1-octanol with dissolved catalyst, saturated with water, was used as solvent phase. The solvent with highest fraction of 1-octanol in previous investigation was the molar ratio of 1-octanol : *n*-undecane = 1.5 : 1, which equals to a molar excess of 1-octanol of 1.5. In the present investigation a molar excess of approximately 5-6 was used due to undiluted 1-octanol. The relative decrease of the concentration of 1-octanol is low enough to assume a constant concentration. Constant concentrations do not contribute to rate law and are included in the rate constants.

Performances of DBSA and $NiDBSA_2$ are already investigated and compared in previous investigation. A practicable characteristic parameter for comparison is the turnover number, which is the molar ratio of product to catalyst. DBSA appeared to be a more efficient catalyst because of its higher turnover number. However, $NiDBSA_2$ shows insolubility in water which is an advantage for separation and purifying of the aqueous phase afterwards. Co-extraction of water could be crucial if change of volume must be considered. In previous research the order of catalyst was determined as 0.4 at 60 °C [1]. This is almost only half of the value, determined in this task. Although, variances in temperature were found in this investigation (Table 12). Thus, more data would be needed to gain certainty about this issue.

In literature, kinetic models for micellar reaction exist based on Michaelis-Menten model for enzyme kinetics [12, 26, 27, 28]. These models use agglomeration numbers, micellar volumes and the respective CMC as parameters. These parameters could be generally determined by surface tension [18, 29, 30, 31], but useful data for determining agglomeration number, micellar volume or CMC could not be generated for this system. Another possible way for determining these parameters would be isothermal titration calorimetry [33] or molecular dynamic simulations [34]. During reaction, parameters like agglomeration number or micellar volume may change, which would be very difficult to measure anyway. As a major drawback, these kinetic models also do not consider reversible reactions. Reaction kinetics of monophasic

esterification of acetic acid and ethanol or methanol is researched with stoichiometric feeds and considering activity coefficients [34, 35]. Extending the model by activity coefficients could increase accuracy, but especially for biphasic systems including metallosurfactants the determination of such coefficients is challenging.

7 Conclusion and Outlook

The initially formulated research question, if a monophasic kinetic model is applicable for describing the reactive extraction of dilute acetic acid is possible, can be answered with 'yes'.

During the present investigations, $NiDBSA_2$ has proven to be an effective catalyst for the biphasic esterification. The monophasic kinetic modeling of the investigated system is applicable at any temperature. High mass fractions of catalyst reduce interfacial tension enough to assume a quasi-monophasic behavior of the system.

To reduce high error in mass balance, the experimental procedure needs revision. The model was tested for the initial concentration of 1 mol L^{-1} of acetic acid in the aqueous phase. As the chosen approach of a monophasic model has shown promising results, an extension to a broader range of initial conditions should be pursued. The order of catalyst was determined for catalyst mass fractions of 5 wt% and 20 wt%. More catalyst loads within this range should be analyzed. The preparation of the catalyst is a crucial step within this investigation, as slight quality differences could cause high deviations.

An in-depth analysis of the system with further variation of the experimental parameters (e.g., phase ratio, initial conditions) requires application of statistical experiment design. Design of experiments has shown high potential especially for multi-parameter systems as in the present case. A variation of this parameter and its effects is interesting to optimize the process for upscaling and continuous operation. Thus, a fundamental understanding of the reaction and extraction process and how they interact is crucial for a scale-up.

Optimization of the mixing during the biphasic esterification could reduce mass balance errors and increase the overall process performance. If the introduced shear forces are too high, unintended emulsification, stable emulsions or foaming could occur. The metallosurfactant catalyst significantly reduces the required mixing energy for a quasi-monophasic state. Analysis on mixing could not be done with the equipment used in this investigation. In addition to the overall optimization, a transfer to CFD simulations is proposed [37].

Bibliography

[1] A. Toth, S. Schnedl, D. Painer, M. Siebenhofer, and S. Lux, "Interfacial catalysis in biphasic carboxylic acid esterification with a nickel-based metallosurfactant," *ACS Sustain. Chem. Eng.*, vol. 7, no. 22, pp. 18547–18553, 2019.

[2] P. Serp, P. Kalck, P. Torrence, and C. Le Berre, *Ullmann's Encylopedia of Industrial Chemistry; Acedic acid*, 7th ed., no. Lcc. Weinheim: Wiley-VCH Verlag GmbH & Co. KGaA, 2013.

[3] V. D. Talnikar and Y. S. Mahajan, "Recovery of acids from dilute streams : A review of process technologies," *Korean J. Chem. Eng*, vol. 31, no. 10, pp. 1720–1731, 2014.

[4] K. Brust, "Toxicity of aliphatic amines on the embryos of zebrafish Danio rerio - experimental studies and QSAR," Technische Universtität Dresden, 2001.

[5] T. G. Bekele, H. Zhao, Q. Wang, and J. Chen, "Bioaccumulation and Trophic Transfer of Emerging Organophosphate Flame Retardants in the Marine Food Webs of Laizhou Bay, North China," *Environ. Sci. Technol.*, vol. 53, no. 22, pp. 13417–13426, 2019.

[6] A. Toth, S. Lux, D. Painer, and M. Siebenhofer, "Reaction Chemistry & Engineering Intensification of esterification through emulsification : isolation of dilute low molecular weight carboxylic acids," *React. Chem. Eng.*, vol. 3, pp. 905–911, 2018.

[7] M. Kienberger, M. Hackl, and M. Siebenhofer, "Recovery of acetic acid using esterification of acetic acid with n-octanol in a membrane reactor," *J. Environ. Chem. Eng.*, vol. 6, no. 2, pp. 3161–3166, 2018.

[8] A. Toth, "Emulsion-Enhanced Biphasic Esterification: Applied Reactive Seperations for Valorization of Dilute Carboxyl Acids," Graz University of Technology, 2019.

[9] T. J. L. Lécrivain, "Investigation on the Diluent Effect on Solvent Extraction Processes of Trivalent f-Elements by Di-Alkyl Organophosphorus Extractants," Washington State University, 2019.

[10] D. R. Lide and G. Baysinger, *CRC Handbook of Chemistry and Physics*, Internet V. Boca Raton, Fl.: CRC Press, 2005.

[11] G. A. Iglesias-silva, A. Gúzma-López, and G. Péréz-Durán, "Densities and Viscosities for Binary Liquid Mixtures of n-Undecane + 1-Propanol, + 1-Butanol, + 1-Pentanol, and + 1-Hexanol from 283.15 to 363.15 K at 0.1 MPa," *J. Cemical Eng. Data*, vol. 61, pp. 2682–2699, 2016.

[12] M. Niyaz Khan, *Micellar Catalysis*, Surfactant. Boca Raton, Fl.: Taylor & Francis Group, 2007.

[13] C. Tanfordl, "Micelle Shape and Size," *J. Phys. Chem.*, vol. 76, no. 21, pp. 3020–3024, 1972.

[14] T. Dwars, E. Paetzold, and G. Oehme, “Reactions in Micellar Systems Angewandte,” *Angewadte Chemie Int. Ed.*, vol. 44, pp. 7174–7199, 2005.

[15] T. F. Tadros, *Emulsion Formation and Stability*, 1st ed. Singapore: Wiley-VCH Verlag GmbH & Co. KGaA, 2013.

[16] J. Short, J. Roberts, D. W. Roberts, G. Hodges, S. Gutsell, and R. S. Ward, “Practical methods for the measurement of log P for surfactants,” *Ecotoxicol. Environ. Saf.*, vol. 73, no. 6, pp. 1484–1489, 2010.

[17] E. Parera, F. Comelles, R. Barnadas, J. Suades, and J. Suades, “New Surfactant Phosphine Ligands and Platinum (II) Metallosurfactants . Influence of Metal Coordination on the Critical Micelle Concentration and Aggregation Properties,” *Langmuir*, vol. 26, no. 13, pp. 743–751, 2010.

[18] P. F. Garrido, P. Brocos, A. Amigo, L. Garciá-Fadrique, and Á. Piñeiro, “STAND: Surface Tension for Aggregation Number Determination,” *Langmuir*, vol. 32, no. 16, pp. 3917–3925, 2016.

[19] S. Ikeda, M. Tsunoda, and H. Maeda, “The Application of the Gibbs Adsorption Isotherm to Aqueous Solutions of a Nonionic-Cationic Surfactant,” *J. Colloid Interface Sci.*, vol. 67, no. 2, pp. 336–348, 1978.

[20] H. Matthias, *Ullmann’s Ecyclopedia of Industrial Chemistry; Microemulsions*, 7th ed. Wiley-VCH Verlag GmbH & Co. KGaA, 2013.

[21] F. Goodarzi and S. Zendehboudi, “A Comprehensive Review on Emulsions and Emulsion Stability in Chemical and Energy Industries,” *Can. J. Chem. Eng.*, vol. 97, no. 1, pp. 281–309, 2019.

[22] N. Paul, “Theoretische und experimentelle Untersuchungen von Transport- und Grenzflächenphänomenen in mizellaren Flüssig / flüssig-Systemen,” Technischen Universität Berlin, 2014.

[23] J. Ancheyta, *Chemical reaction kinetics : concepts, methods and case studies*, 1st ed. Mexico City: Wiley-VCH Verlag GmbH & Co. KGaA, 2017.

[24] J. Burés, “A Simple Graphical Method to Determine the Order in Catalyst,” *Angewadte Chemie Int. Ed.*, vol. 55, pp. 2028–2031, 2016.

[25] J. Burés, “Variable Time Normalization Analysis : General Graphical Elucidation of Reaction Orders from Concentration Profiles,” *Angewadte Chemie Int. Ed.*, vol. 55, pp. 16084–16087, 2016.

[26] A. Keshav, K. L. Wasewar, and S. Chand, “Desalination and Water Treatment Recovery of propionic acid by reactive extraction - 1 . Equilibrium , effect of pH and temperature , water coextraction,” *Desalt. Water Treat.*, vol. 3, no. 1–3, pp. 91–98, 2009.

[27] A. Cornish-Bowden, “One hundred years of Michaelis – Menten,” *Perspect. Sci.*, vol. 4, pp. 3–9, 2015.

[28] K. M. Park, O. T. Kwon, S. M. Ahn, J. Lee, and P.-S. Chang, “Characterization and optimization of carboxylesterase-catalyzed esterification between capric acid and glycerol for the production of 1-monocaprin in reversed micellar system,” *N. Biotechnol.*, vol. 27, no. 1, pp. 46–52, 2010.

[29] C. Bravo-Díaz *et al.*, “To Model Chemical Reactivity in Heterogeneous Emulsions , Think Homogeneous Microemulsions,” *Langmuir*, vol. 31, no. 33, pp. 8961–8979, 2015.

[30] C. A. Bunton, “Reactivity in aqueous association colloids. Descriptive utility of the pseudophase model,” *J. Mol. Liq.*, vol. 7322, no. 72, pp. 231–249, 1997.

[31] A. I. Rusanov, “Refining of Nonionic Surfactant Micellization Theory Based on the Law of Mass Action,” *Colloid J.*, vol. 78, no. 3, pp. 371–377, 2016.

[32] A. I. Rusanov, “On the Problem of Determining Aggregation Numbers from Surface Tension Measurements,” *Langmuir*, vol. 33, no. 44, pp. 12643–12650, 2017.

[33] N. E. Olesen, P. Westh, and R. Holm, “Determination of thermodynamic potentials and the aggregation number for micelles with the mass-action model by isothermal titration calorimetry : a case study on bile salts,” *J. Colloid Interface Sci.*, vol. 453, pp. 79–89, 2015.

[34] F. Palazzesi, M. Calvaresi, and F. Zerbetto, “A molecular dynamics investigation of structure and dynamics of SDS and SDBS micelles,” *Soft Matter*, vol. 7, no. 19, pp. 9148–9156, 2011.

[35] M. Mekala and V. R. Goli, “Kinetics of esterification of methanol and acetic acid with mineral homogeneous acid catalyst,” *CJCHE*, vol. 23, no. 1, pp. 100–105, 2015.

[36] C. Beula, “Kinetics of Esterification of Acetic Acid and Ethanol with a Homogeneous Acid Catalyst,” *Indian Chem. Eng.*, vol. 57, no. 2, pp. 177–196, 2014.

[37] S. F. Roudsari, G. Turcotte, R. Dhib, and F. Ein-Mozaffari, “CFD modeling of the mixing of water in oil emulsions,” *Comput. Chem. Eng.*, vol. 45, pp. 124–136, 2012.

List of Figures

List of Tables

Appendix

A Diagrams of molar load

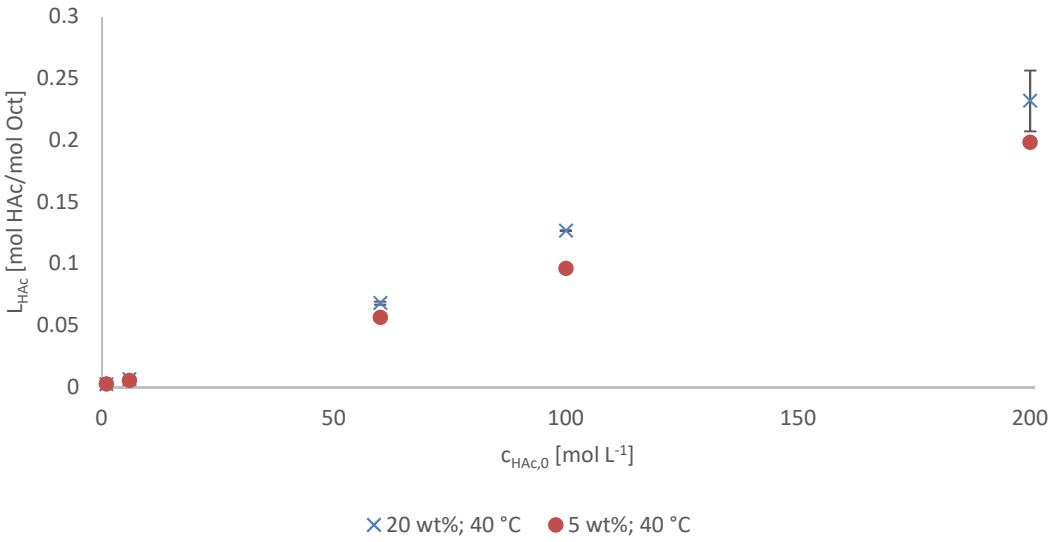

Figure 34: comparison of molar loads of acetic acid in 1-octanol at 40 °C with 5 and 20 wt% of catalyst; related to initial aqueous concentration of acetic

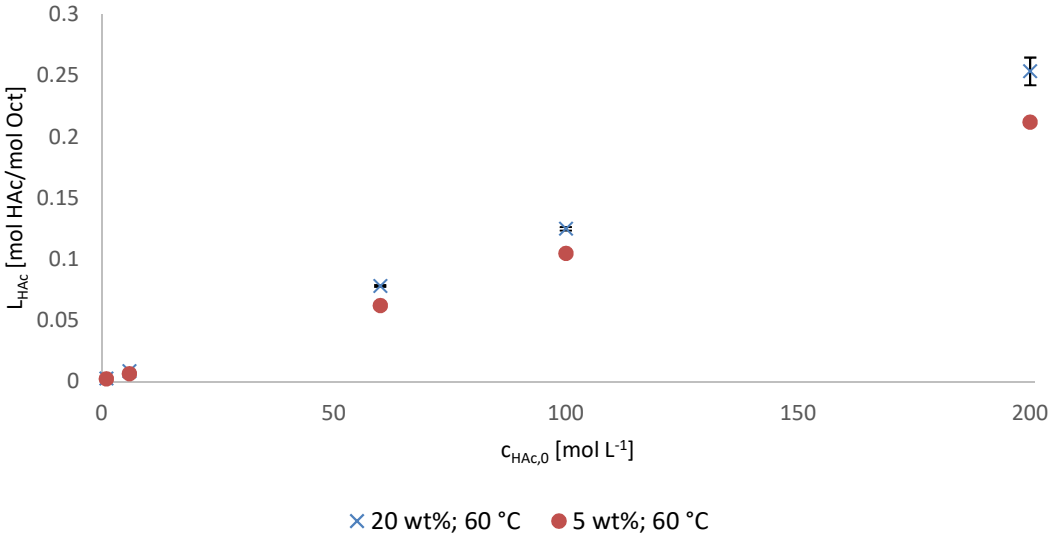

Figure 35: comparison of molar loads of acetic acid in 1-octanol at 60 °C with 5 and 20 wt% of catalyst; related to initial aqueous concentration of acetic

B Diagrams for determination of distribution coefficient

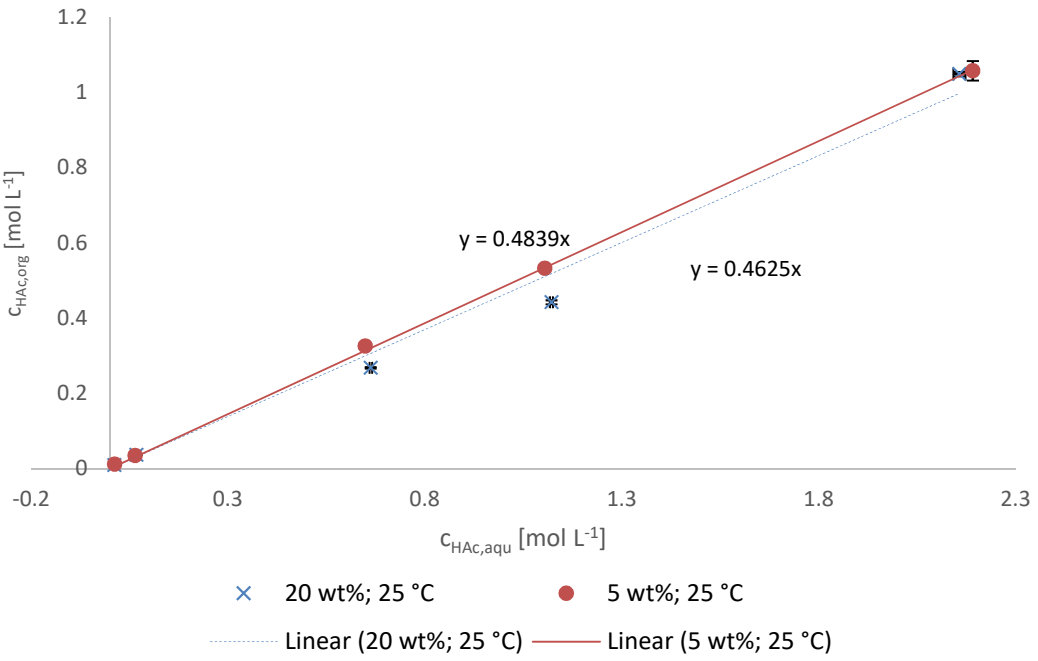

Figure 36: Determination of the distribution coefficient as slope in linear regression; 25 °C with 5 and 20 wt% catalyst

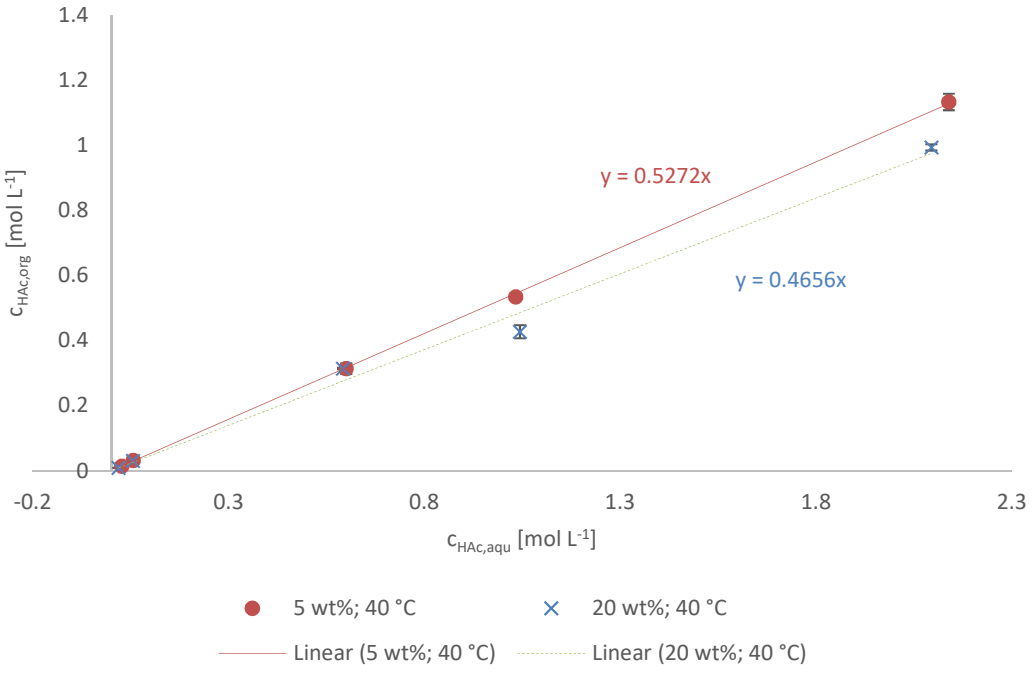

Figure 37: Determination of the distribution coefficient as slope in linear regression; 40 °C with 5 and 20 wt% catalyst

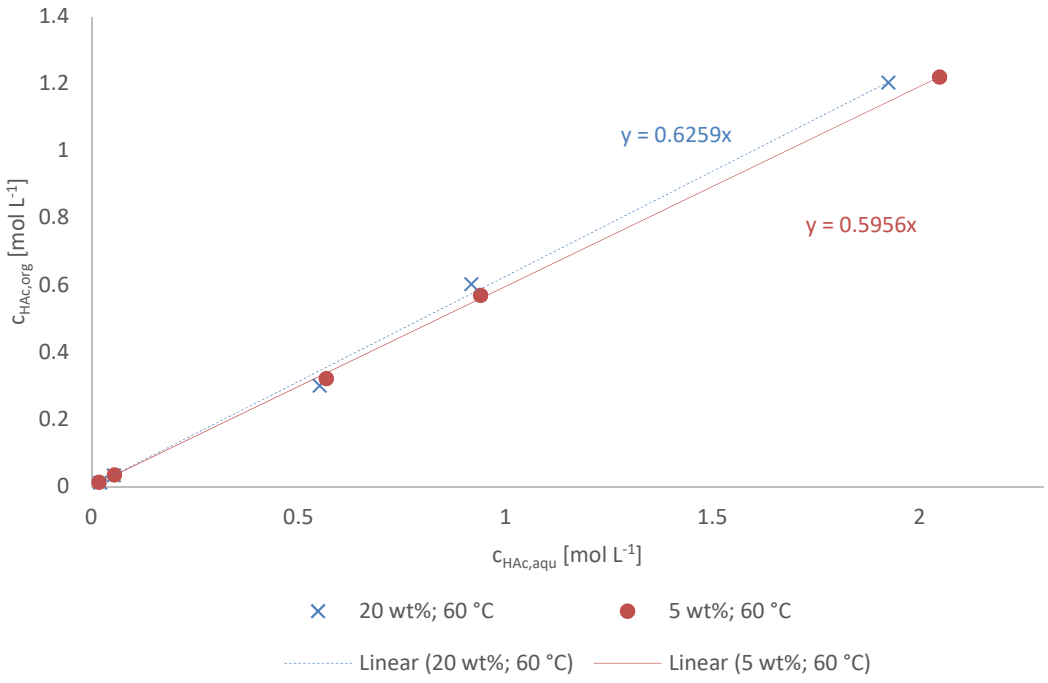

Figure 38: Determination of the distribution coefficient as slope in linear regression; 60 °C with 5 and 20 wt% catalyst

C Kinetic modeling

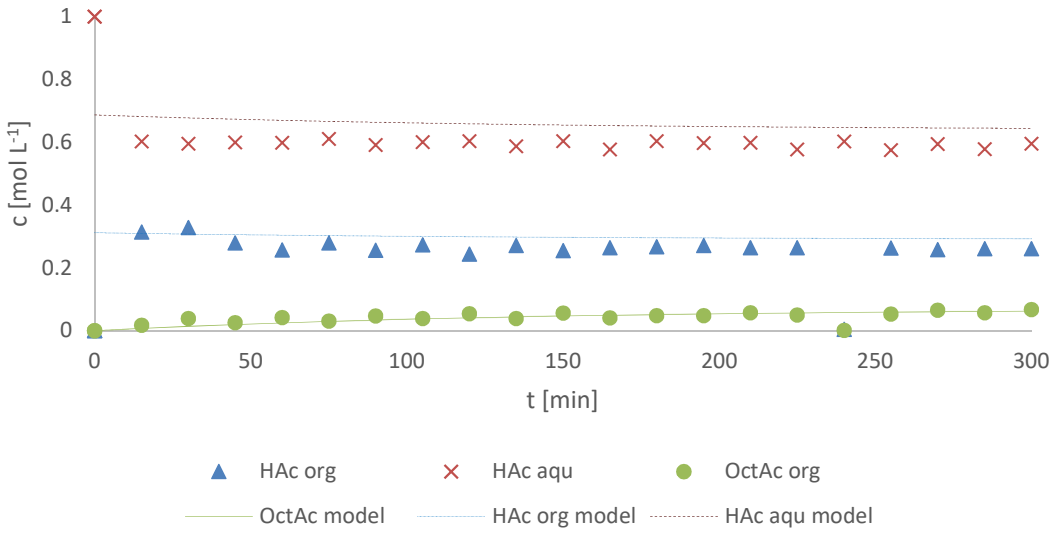

Figure 39: Concentration profiles of acetic acid in aqueous and organic phase and octyl acetate in organic phase, compared with their modeled concentrations at 25 °C and 5 wt% catalyst

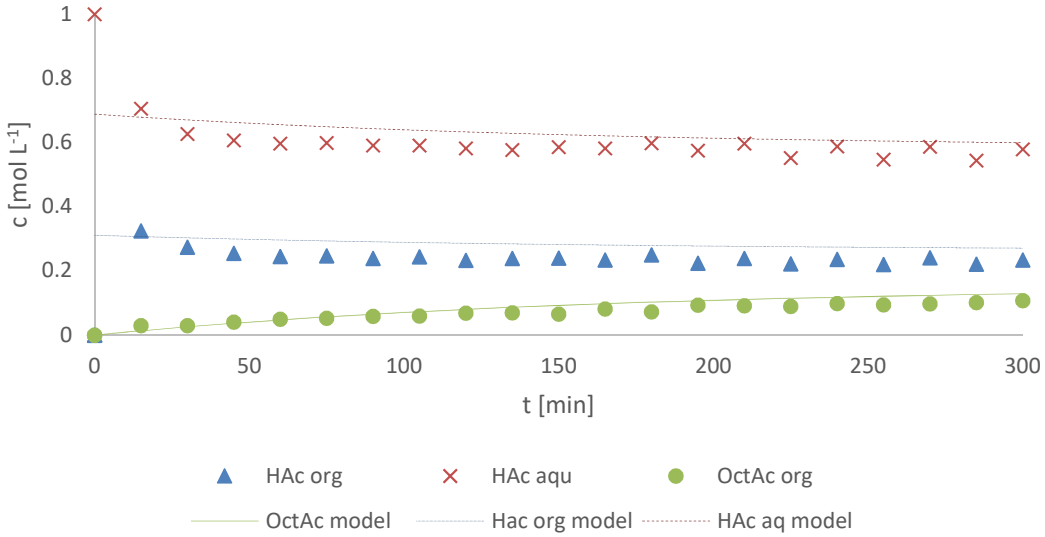

Figure 40: Concentration profiles of acetic acid in aqueous and organic phase and octyl acetate in organic phase, compared with their modeled concentrations at 25 °C and 20 wt% catalyst

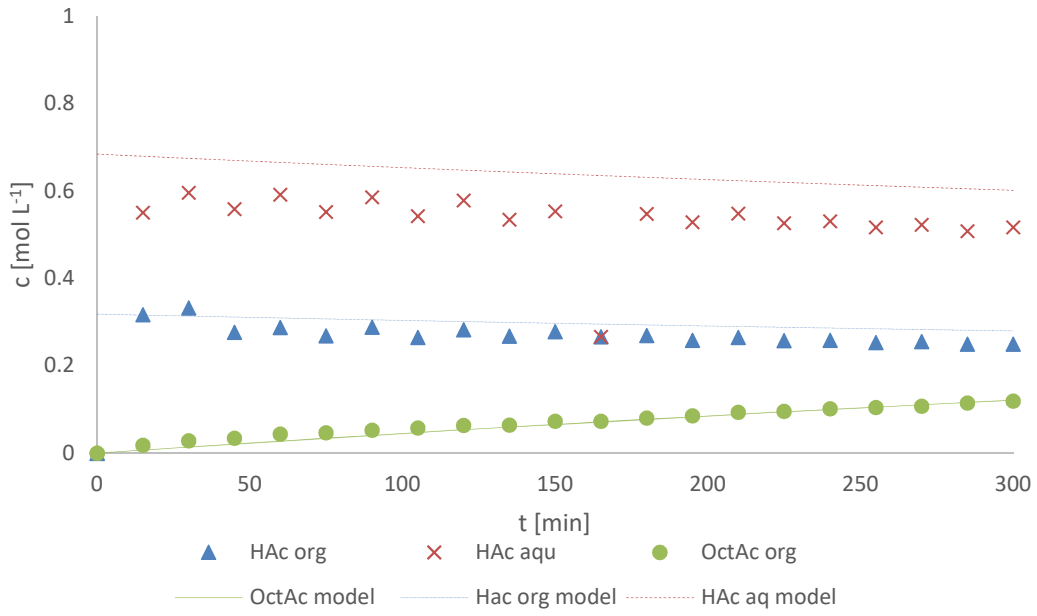

Figure 41: Concentration profiles of acetic acid in aqueous and organic phase and octyl acetate in organic phase, compared with their modeled concentrations at 40 °C and 5 wt% catalyst

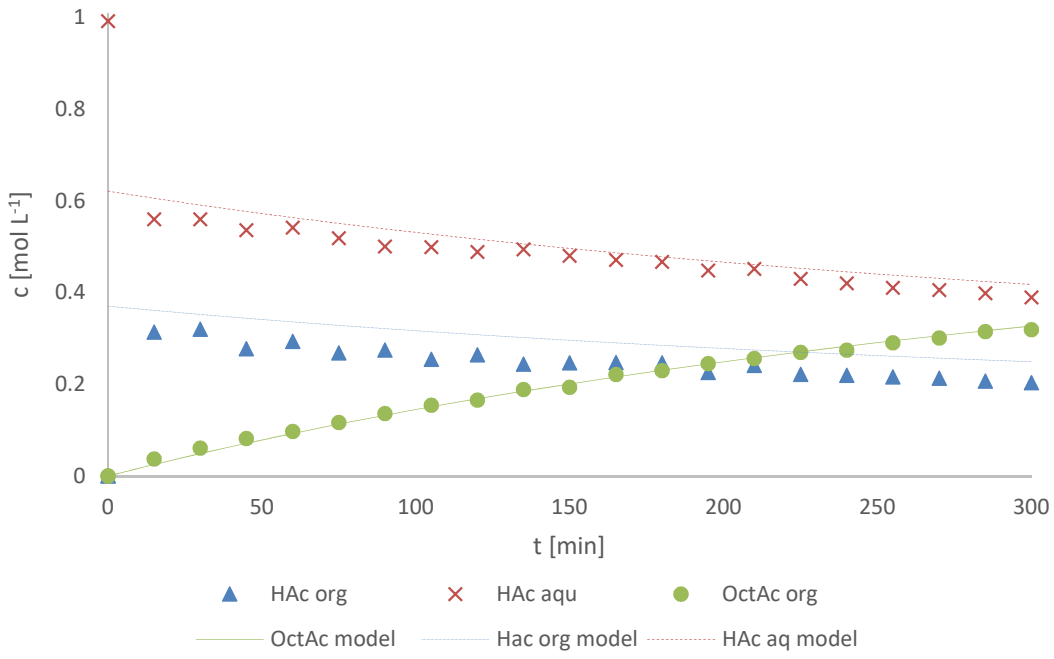

Figure 42: Concentration profiles of acetic acid in aqueous and organic phase and octyl acetate in organic phase, compared with their modeled concentrations at 60 °C and 5 wt% catalyst

D Order of catalyst

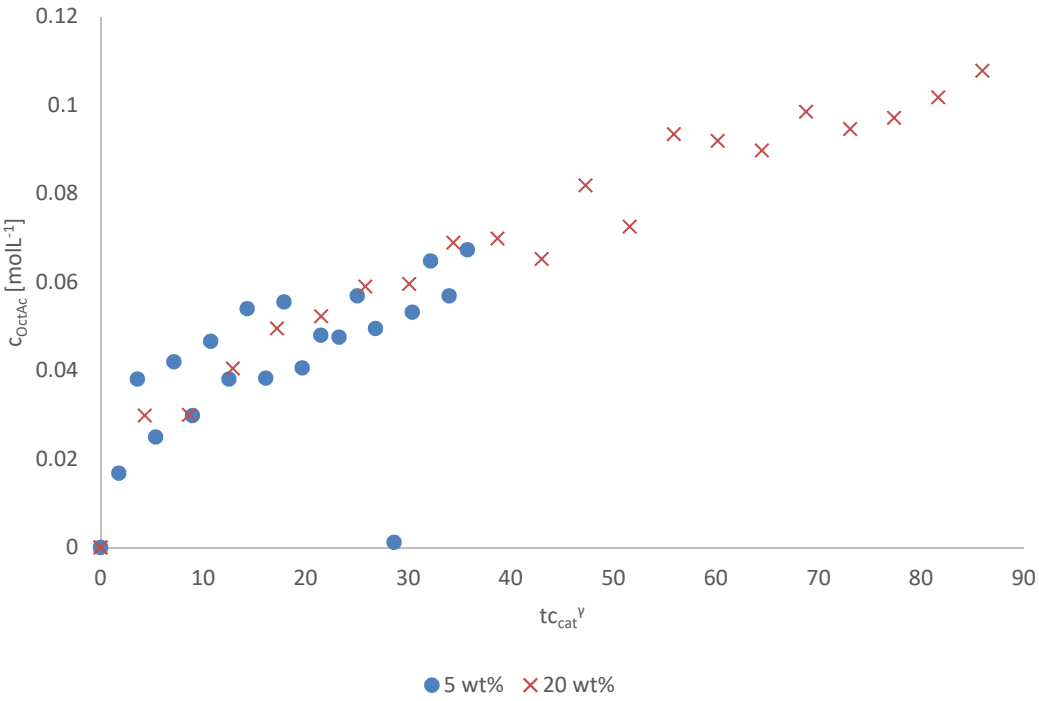

Figure 43: Determination of order of catalyst γ; time-normalized abscissa at 25 °C

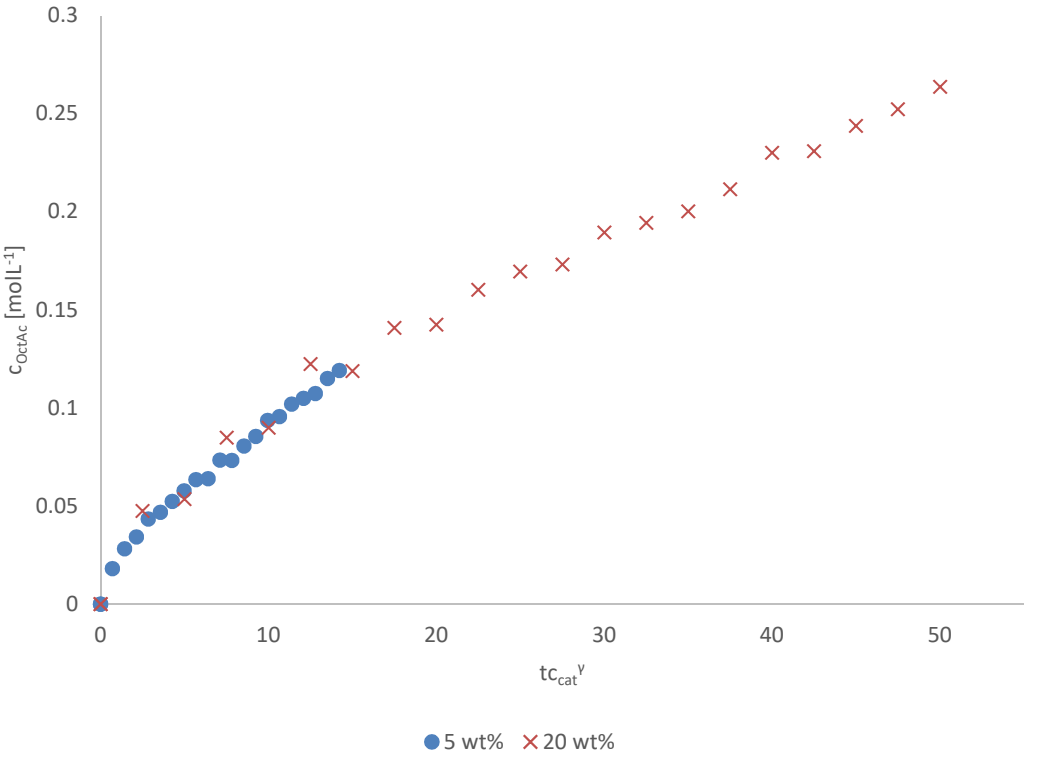

Figure 44: Determination of order of catalyst γ; time-normalized abscissa at 40 °C